(2 C)

SOIL-STRUCTURE INTERACTION ANALYSIS OF QUARTER SCALE MODEL USING AXERA CODE

T. Sato*, S. Nakai**, F. Yamazaki**, A. Mita** and T. Ishii#

INTRODUCTION

Lotung SSI research project was initiated by the Electric Power Research Institute (EPRI), the US Nuclear Regulatory Commission (NRC) and the Taiwan Power Company (TPC). Based on the technical exchange agreement between EPRI and the Tokyo Electric Power Company (TEPCO), TEPCO sponsored the analytical investigation of the Lotung experiment in Japan. Ohsaki Research Institute (ORI) participated in this project as one of the contractors of TEPCO and conducted the prediction analysis and correlation assessment whose flow chart is shown in Fig. 1. This workshop paper presents research results and findings obtained through the analysis using the computer code AXERA (Axisymmetric Earthquake Response Analysis). Note that ORI also employed another analysis method using the computer code HYBAX. The detailed flow charts of the prediction and correlation studies for the forced vibration test (FVT) and the actual earthquake records (May 20, 1986 and November 14, 1986) are shown in Figs. 2 and 3, respectively. A schematic view of the analysis method used in this paper is depicted in Fig. 4. AXERA based on an axisymmetric finite element method can deal with both substructure and direct approaches. In the present study, the direct approach is chosen. AXERA is similar to ALUSH except that AXERA allows an introduction of viscous boundaries (dashpots) on the bottom surface.

The analysis matrix of the current work is shown in Table 1 in which only the properties of the upper portion of the layered soil model and the backfill are depicted since the lower portion was not changed throughout the analysis. Based on the soil data packages, model B has been constructed for FVT blind prediction. Since the elastic wave velocities of the backfill are not given, they were assumed in the modeling. Through the comparison between the prediction and FVT measurement, model C has been constructed. These models B and C have been used for the blind prediction of responses subjected to May 20, 1986 earthquake. In the earthquake response analysis, the computer code SHAKE (1) was utilized to obtain the free-field in-ground motion and to construct equivalent linear soil models. Model C' has further constructed through the comparison between the earthquake response prediction and recorded motions. The response prediction for November 14, 1986 earthquake has been finally carried out using the model C'.

* Chief Research Engineer, Ohsaki Research Institute, Inc.
** Chief Research Engineer, Ohsaki Research Institute, Inc., Ph. D./Dr. Eng.
# Research Engineer, Ohsaki Research Institute, Inc.

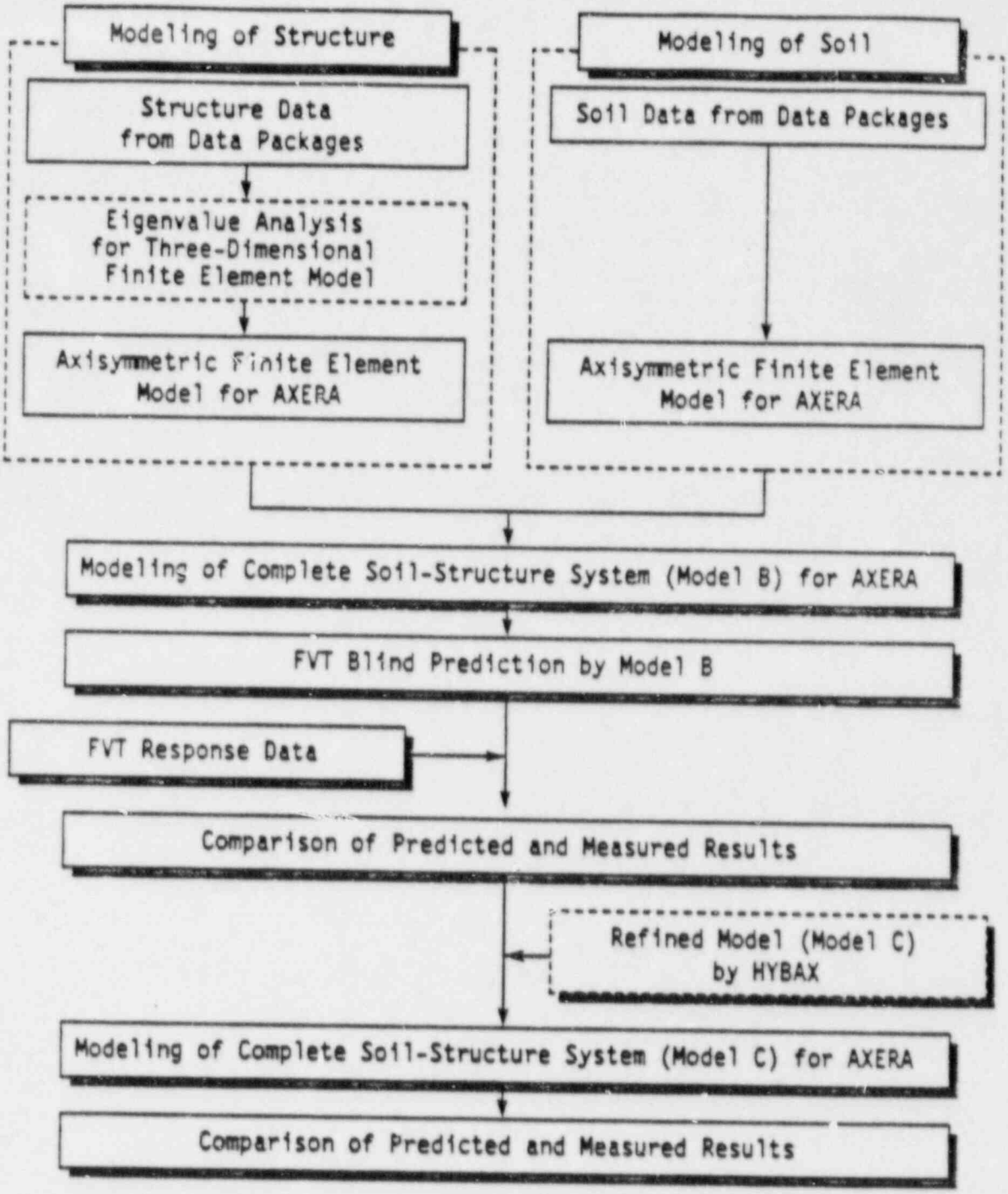

Figure 2. Flow Chart of FVT Prediction and Correlation Analysis

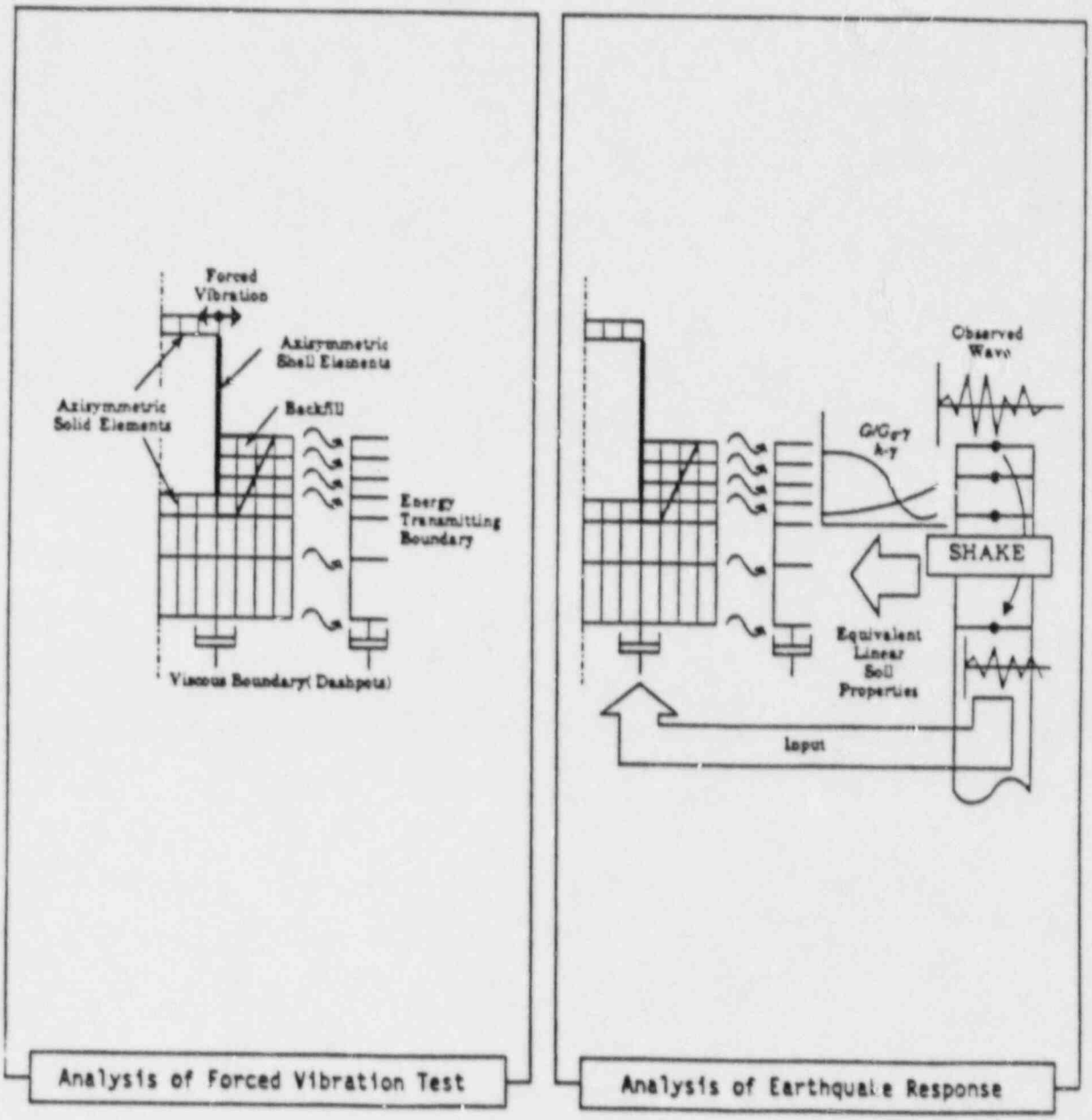

Figure 4. Analysis Metnod of AXERA

MODEL DEVELOPMENT AND DESCRIPTION

Soil Modeling

Soil properties of Lotung SSI experiment site were summarized out of the geological exploration and soil testing reports (Data Packages a, e and f). The soil modeling (Table 2) was determined primarily based on the result of cross-hole shootings (set of L2, L5, L6 and L7 holes). Since there are no measured data for the backfill, the S-wave velocity V_s and the P-wave velocity V_p were assumed for the blind prediction of FVT. The saturated unit weight is employed for all the soil layers (except for the backfill in model B) because the water table is considered to be high (W.L.= GL±0).

A nonlinear soil model was constructed based on the soil testing report (Data Package h) which contains results of resonant column tests and cyclic triaxial tests for undisturbed and remolded soil specimens. These test data were plotted in the equivalent linear representation (shear modulus reduction ratio G/G_0 vs. shear strain γ, and damping ratio h vs. shear strain γ) for five confining pressures, σ_c=0.35, 0.5, 1.0, 2.0, 3.5 kg/cm^2. Then the following hyperbolic relationship between G/G_0 and γ was introduced:

$$\frac{G}{G_0} = \frac{1}{1 + \frac{\gamma}{\gamma_r}} \qquad \cdots\cdots\cdots (1)$$

in which γ_r is the reference strain when G/G_0=0.5. It is well-known that the reference strain becomes large as the confining pressure increases. Thus three values of γ_r were used in the modeling according to the confining pressure as shown in Fig. 5. The damping ratio h was modeled as

$$h = h_{max}\left(1 - \frac{G}{G_0}\right) + h_0 = h_{max} \cdot \frac{\frac{\gamma}{\gamma_r}}{1 + \frac{\gamma}{\gamma_r}} + h_0 \qquad \cdots\cdots\cdots (2)$$

in which h_{max} is the damping ratio at infinitely large strain and h_0 is the initial damping ratio added to the linear relationship in order to avoid infinitesimal value of h. In this study, these parameters for the damping ratio were determined as h_{max}=0.3 and h_0=0.015 for all the soils based on the laboratory test results. The soil region below GL-80m was assumed to be a linear elastic half-space.

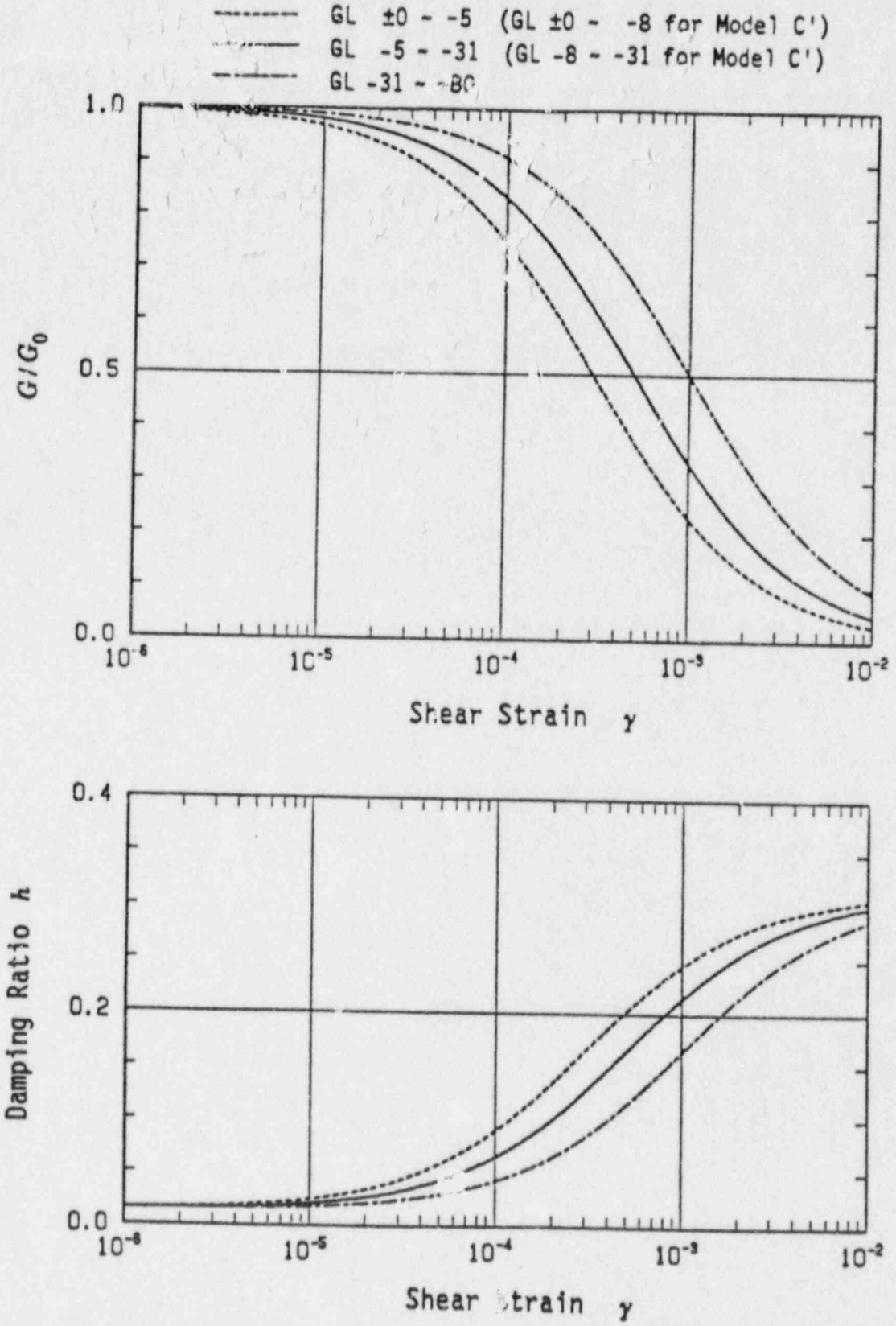

Figure 5. Model for Strain-Dependent Soil Properties

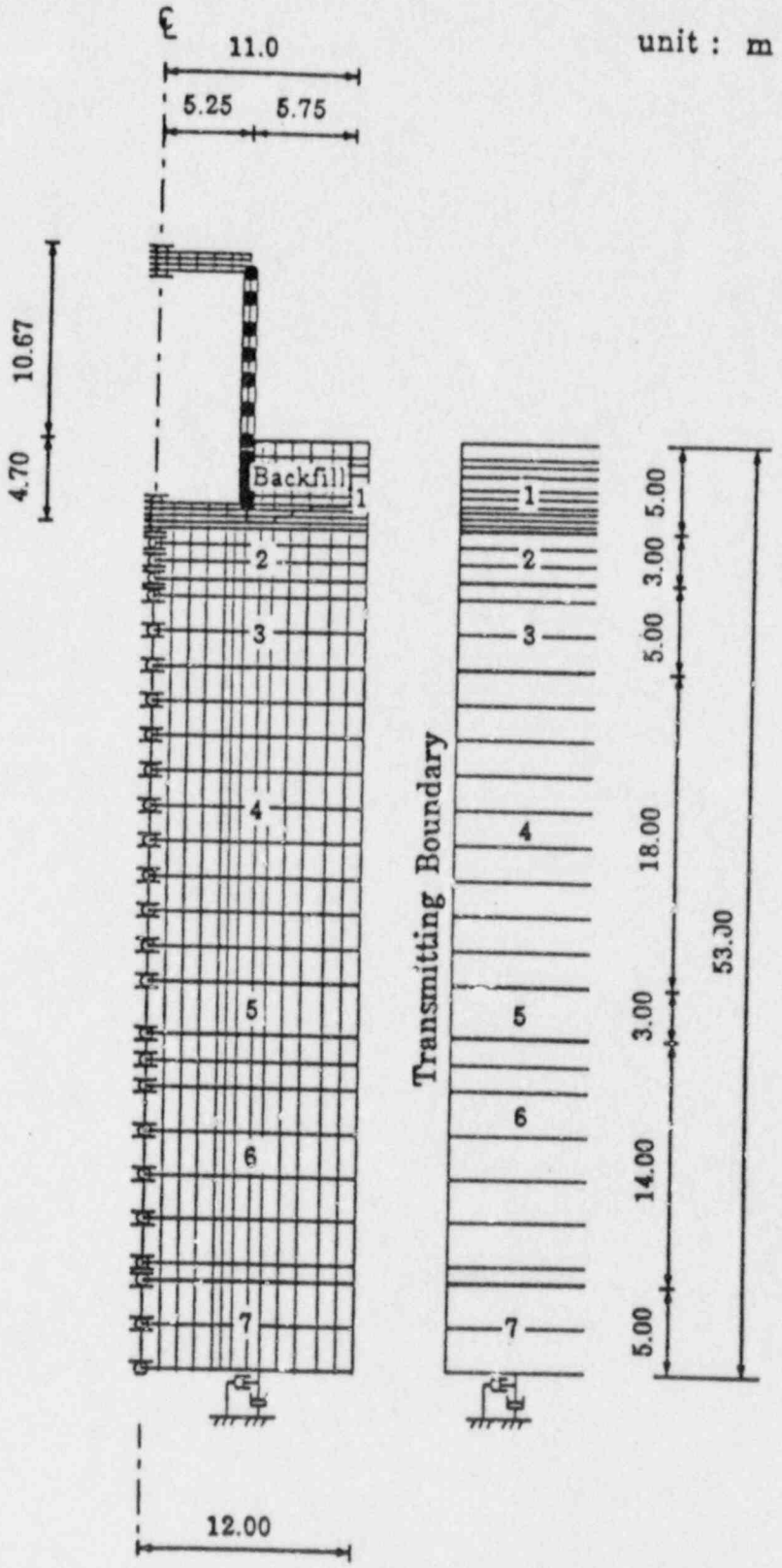

Figure 6. Axisymmetric Model Layout for AXERA

Table 4

Comparison of System Frequency and Damping

		System Frequency f_o (Hz)	Damping Coefficient h (%)
FVT	(radial)	3.80	9.5
	(tangential)	3.81	11.0
Blind Prediction	(model B)	4.25	11.6
Correlation Analysis	(model C)	3.98	14.0

Vibration Modes

The vibration modes at the system frequency of the first rocking modes for the radial and tangential excitation tests have been identified and they are presented in Fig. 11 using a vector representation, which includes both the amplitude and phase information. The rocking components due to the rotation of the base were obtained from the vertical response values recorded at the edge of the base assuming it to be rigid.

Comparing these mode shapes, it has been confirmed that the vibration modes predicted by the Phase I analysis agree well with those identified from the FVT results and that at the system frequency of the first rocking mode, the containment structure model vibrates almost like a rigid body.

Refined Model C

Comparing the blind prediction and vibration test results, it was found that the model B gave slightly higher system frequency for the first rocking mode. Inspection of the vibration modes and response amplitudes indicated that the containment model might need no modification. Therefore the possible modifications were restricted to the soil properties.

The elastic wave velocities of the soil layers of the model B were determined from the results of the cross-hole shootings as described before. However, for the top soil layer which extends GL±0m to GL-5m and the backfill, it is expected that their surface portions are softer than the assumed soil profile. In addition, since there are no data available to determine the elastic wave velocities of the backfill, the assumed values for the backfill in the blind prediction (Phase I) analysis can be modified. Considering all these, it has been decided to modify

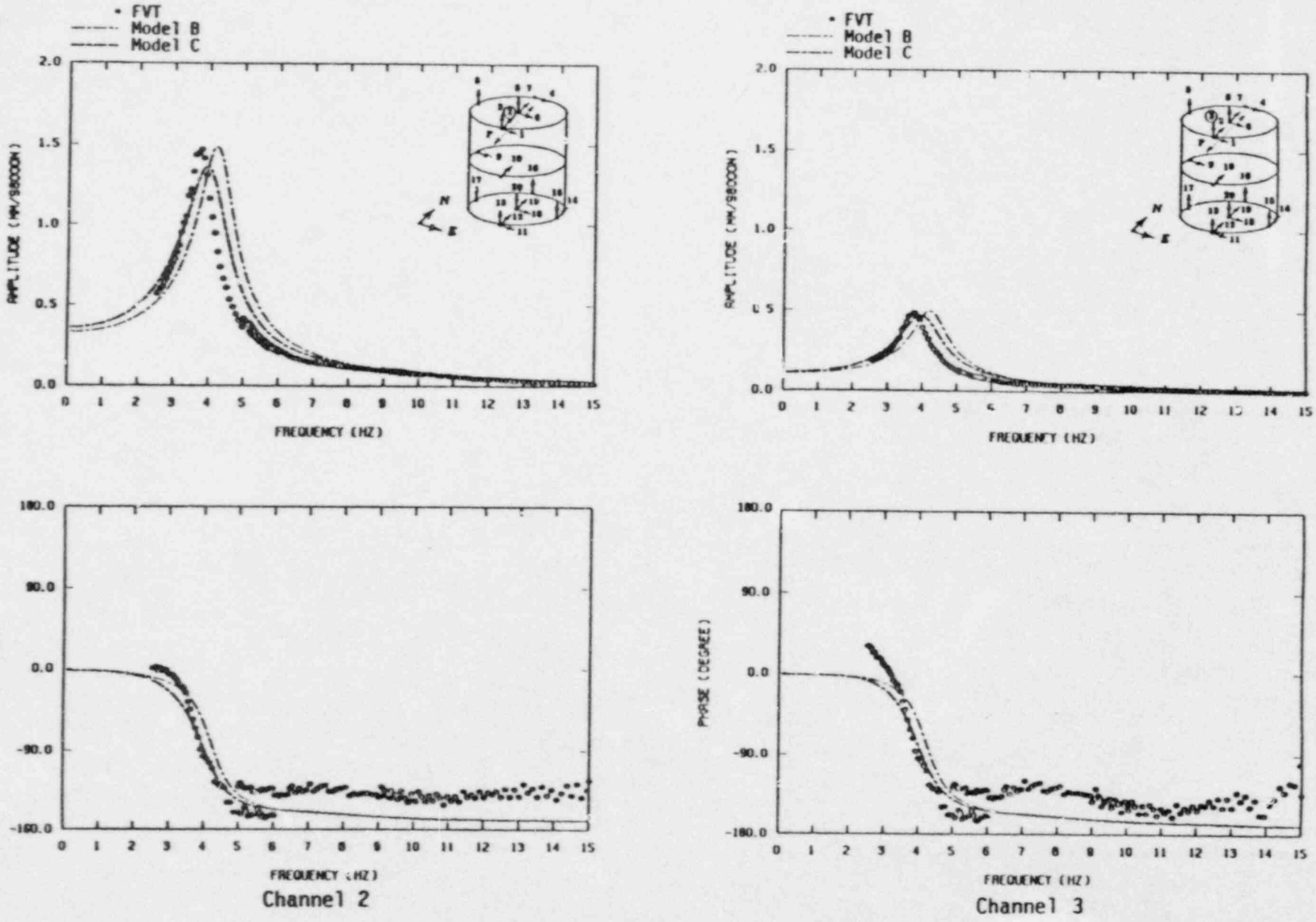

Figure 7. Response to the Radial Excitation (Channel 2,3)

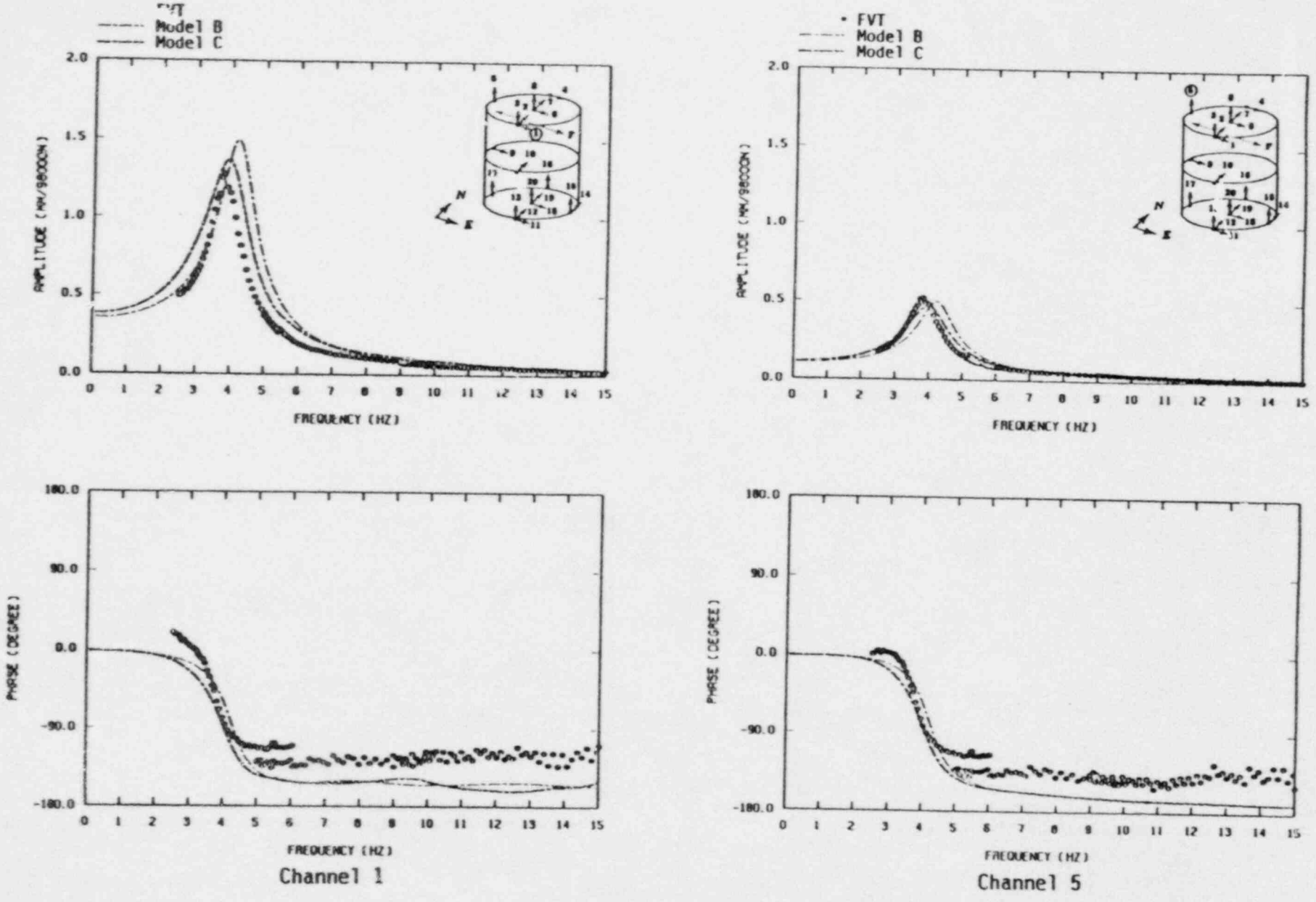

Figure 9. Response to the Tangential Excitation (Channel 1,5)

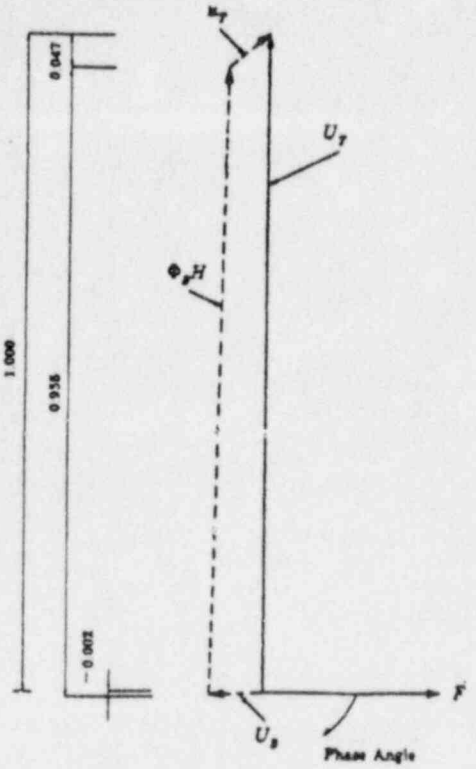

Vibration Test Result
for Radial Excitation
(f_0=3.80Hz)

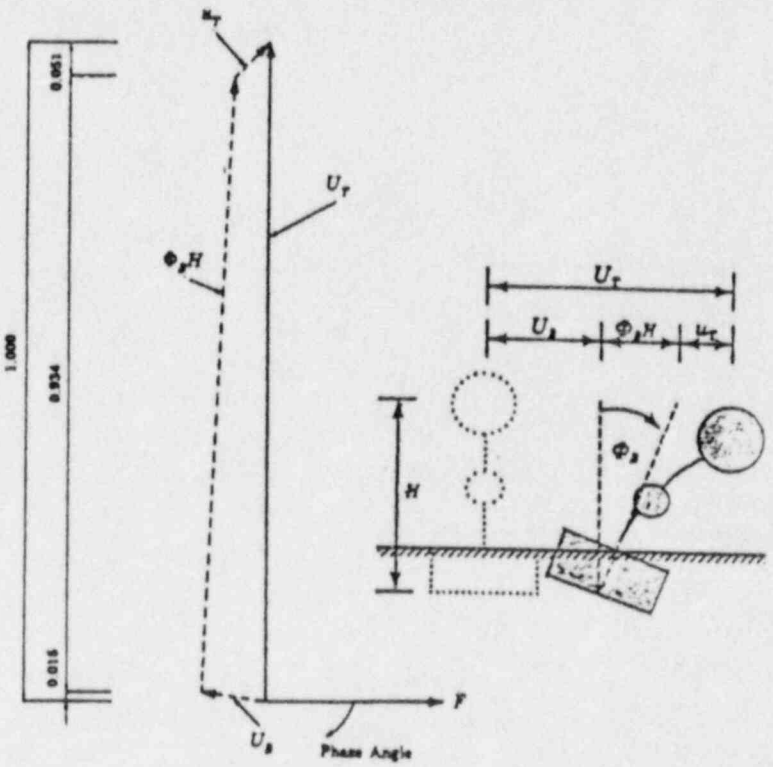

Vibration Test Result
for Tangential Excitation
(f_0=3.81Hz)

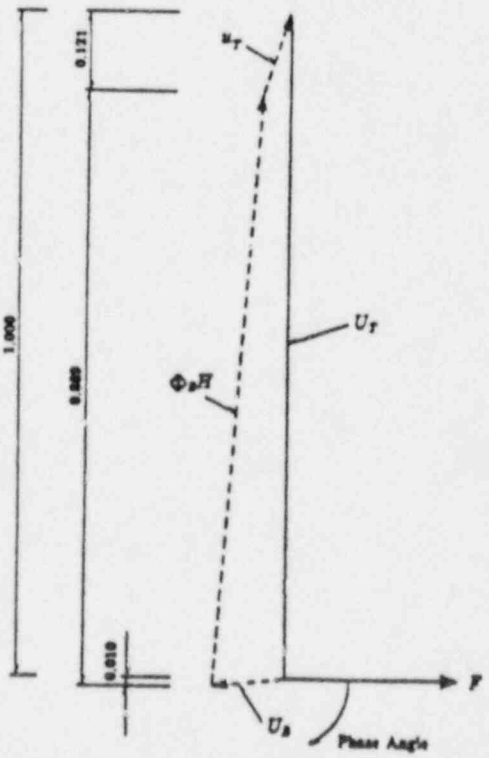

Model B for Radial Excitation
(f_0=4.25Hz)

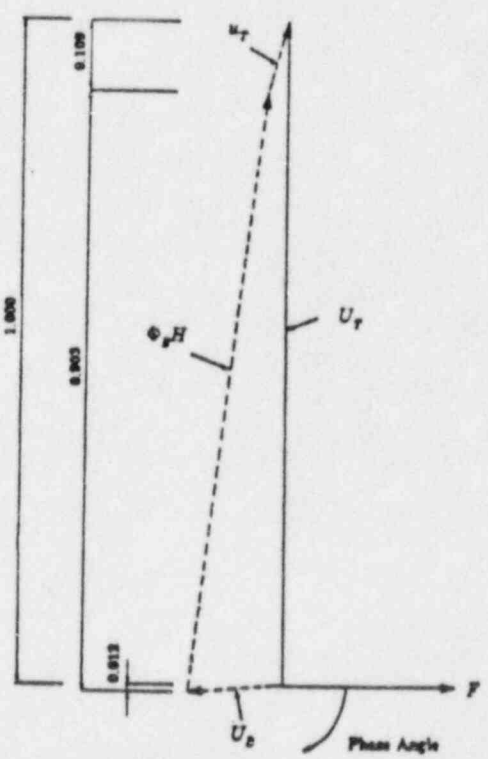

Model C for Radial Excitation
(f_0=3.98Hz)

Figure 11. Vector Representation of Total Response at the Top

V_p was used instead of V_s. All the other conditions of the analysis are the same as those for the N-S and E-W components. The equivalent linear soil properties for the N-S and E-W components obtained by the deconvolution analyses are shown in Fig. 13. In Fig. 14, in-ground distribution of the maximum accelerations to the May 20, 1986 earthquake is depicted. Acceleration response spectra with h=5% at DHB6 and DHB47 are calculated and shown in Figs. 15 and 16, respectively.

Equivalent Linear Soil Models for AXERA

The computer code AXERA is based on a frequency domain analysis and does not deal with nonlinear problems. Hence, equivalent linear soil models were constructed from the analysis results by SHAKE to consider the soil nonlinearity during the earthquake. In the SHAKE analysis two sets of G/G_0 and h values for both N-S and E-W components were obtained. For making the equivalent linear soil models, they were averaged in each soil layer and the resulting models are explained in Table 5 for the models B and C and Table 6 for the model C'. In the above process, the P-wave velocities were kept unchanged over all layers. Though the damping ratios for vertical motion are different from those for the horizontal motion, the damping values for the horizontal motion were employed for the models B and C. The G/G_0 value of the backfill was determined by assuming that the shear stress of the backfill is equal to that of the top soil layer. Therefore the strain of the backfill γ_B was determined by the following equation:

$$\gamma_B = \frac{G_{01}}{G_{0B}} \gamma_1 \qquad \text{..... (3)}$$

where γ_1, G_{0B} and G_{01} represent the strain of the top soil layer, the initial shear modulus of the backfill and that of the top soil layer, respectively. Substituting this γ_B into Eqs. 1 and 2, G/G_0 and h for the backfill were obtained.

Response Analysis Using AXERA

Using the equivalent linear soil models, the frequency response analysis was performed to obtain transfer functions with respect to the control point (FA1-5). The seismic excitations were chosen to be vertically incident plane S-waves for the horizontal excitations and a vertically incident plane P-wave for the vertical excitation. The transfer functions were obtained for the N-S (vertically incident plane S-wave with N-S particle motion), E-W (vertically incident plane S-wave with E-W particle motion) and U-D (vertically incident plane P-wave) excitations.

Time Histories and Acceleration Response Spectra

By use of the transfer functions, the time histories of the response to the May 20, 1986 earthquake were calculated through the FFT algorithm. Since the steam generator was not modeled, the response values at F4GU and F4GL were not obtained.

The 5% acceleration response spectra for the calculated motions and the recorded

Layer No.	Depth G.L. (m)	Sublayer	Location of Accelerometers	V_s (m/sec)
1	0.0 ▽ −5.0		GL±0	120/85*
2	▽ −8.0		GL−6	140*
3	▽ −13.0		GL−11	190
4	▽ −31.0		GL−17	220
5	▽ −34.0			280
6	▽ −48.0		GL−47	250
7	▽ −60.0			270
8	▽ −80.0			320
9	▽ −∞	Elastic Halfspace		480

* V_s values of sublayers in Layer 1 (and 2) are assumed to increase according to depth (See detail in Table 1).

Figure 12. Analysis Model For SHAKE

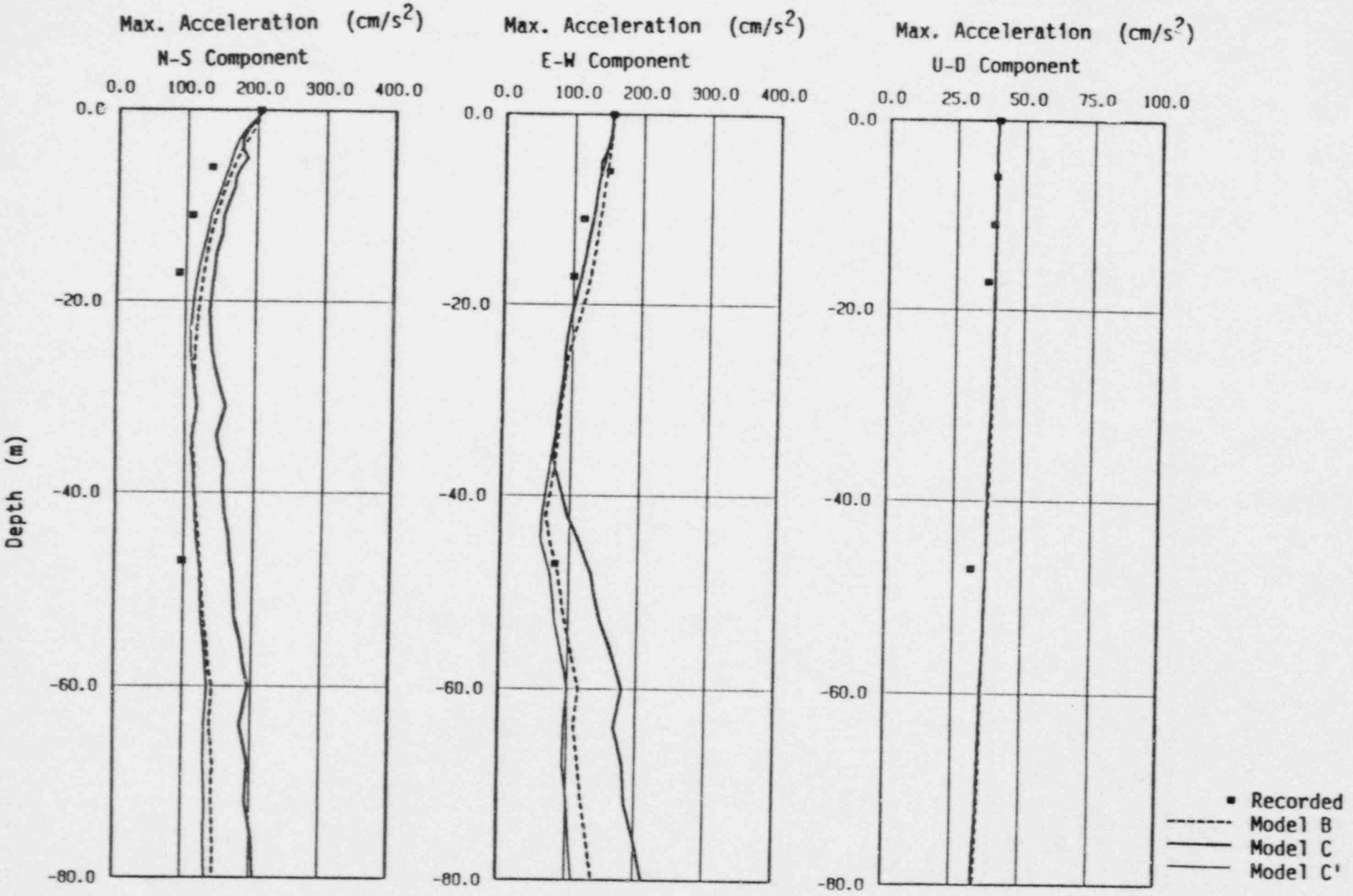

Figure 14. Maximum Ground Acceleration for May 20, 1986 Earthquake

Table 6

Equivalent Linear Soil Model for May 20, 1986 Earthquake (Model C')

Layer No.	Depth G.L. (m)	Reduction Ratio G/G_0	V_s (m/s)	V_p (m/s)	Unit Weight γ_t (t/m^3)	Shear Modulus G (t/m^2)	Poisson's Ratio ν	Damping Ratios h
1	0.0 ▽ -5.0	0.50	60	262	1.87	690	0.472	0.105
2	▽ -8.0	0.50	99	810	1.87	1870	0.492	0.105
3	▽ -13.0	0.75	165	1270	1.87	5160	0.491	0.070
4	▽ -31.0	0.70	184	1330	1.87	6460	0.490	0.080
5	▽ -34.0	0.90	266	1330	1.90	13670	0.479	0.050
6	▽ -48.0	0.85	230	1250	1.90	10290	0.483	0.055
7	▽ -∞	0.85	249	1220	1.90	12000	0.478	0.055

Backfill (inner)	0.0 ▽ -5.0	0.33	60	323	2.24	822	0.482	0.115
Backfill (outer)	0.0 ▽ -5.0	0.65	85	323	2.24	1640	0.463	0.085

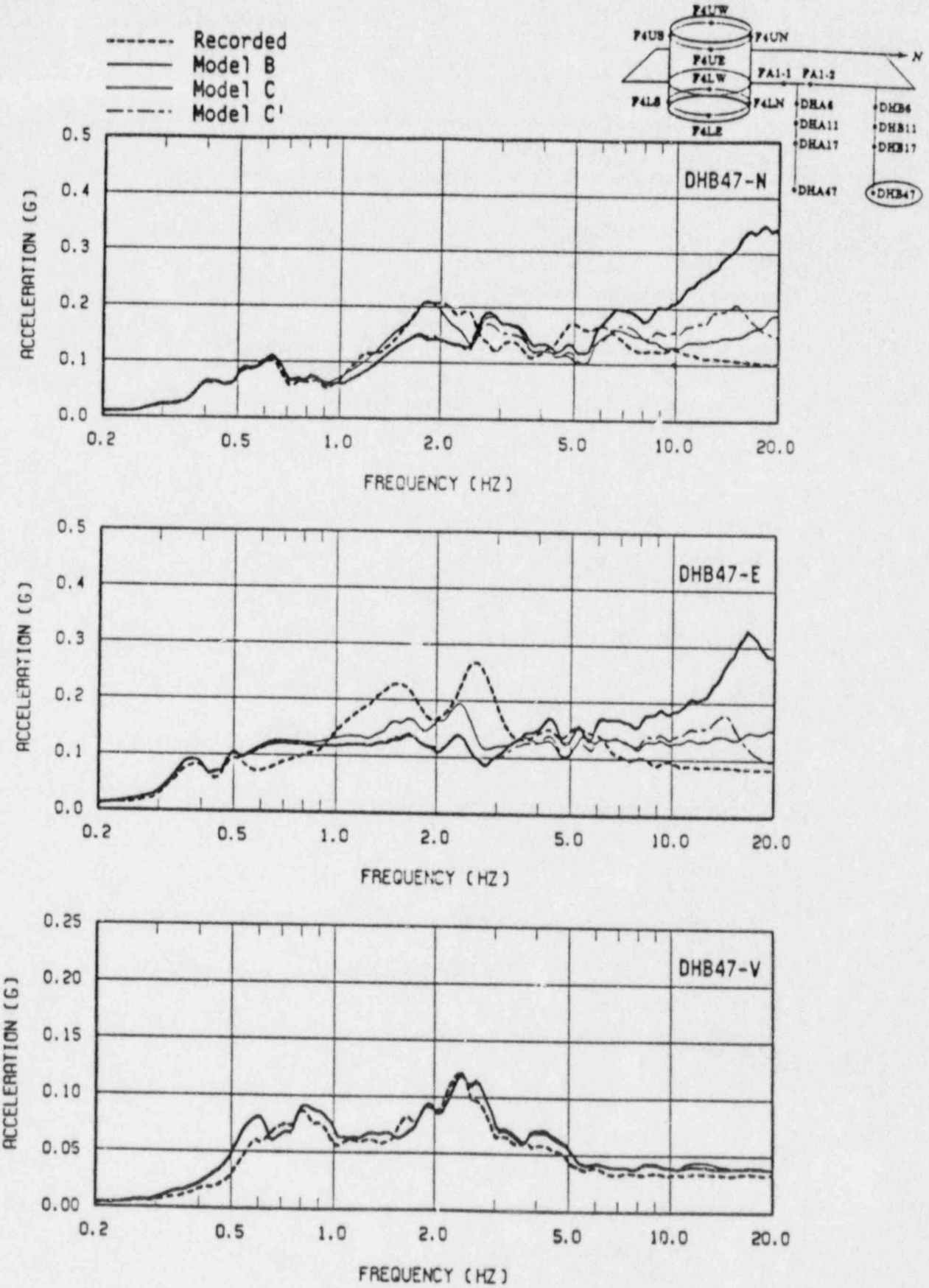

Figure 16. Acceleration Response Spectra at DHB47 for May 20, 1986 Earthquake (h=5%)

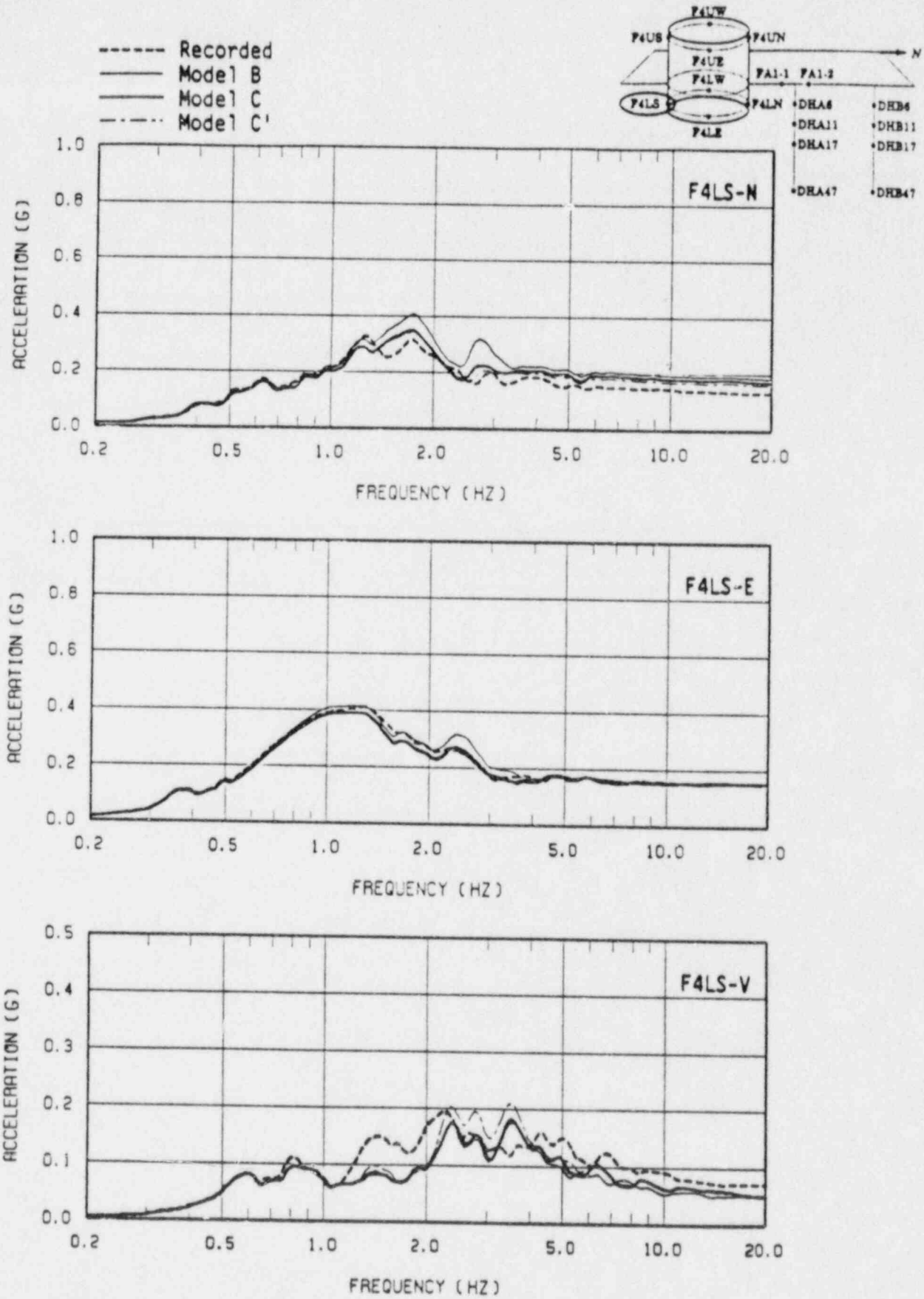

Figure 18. Acceleration Response Spectra at F4LS for May 20, 1986 Earthquake (λ=5%)

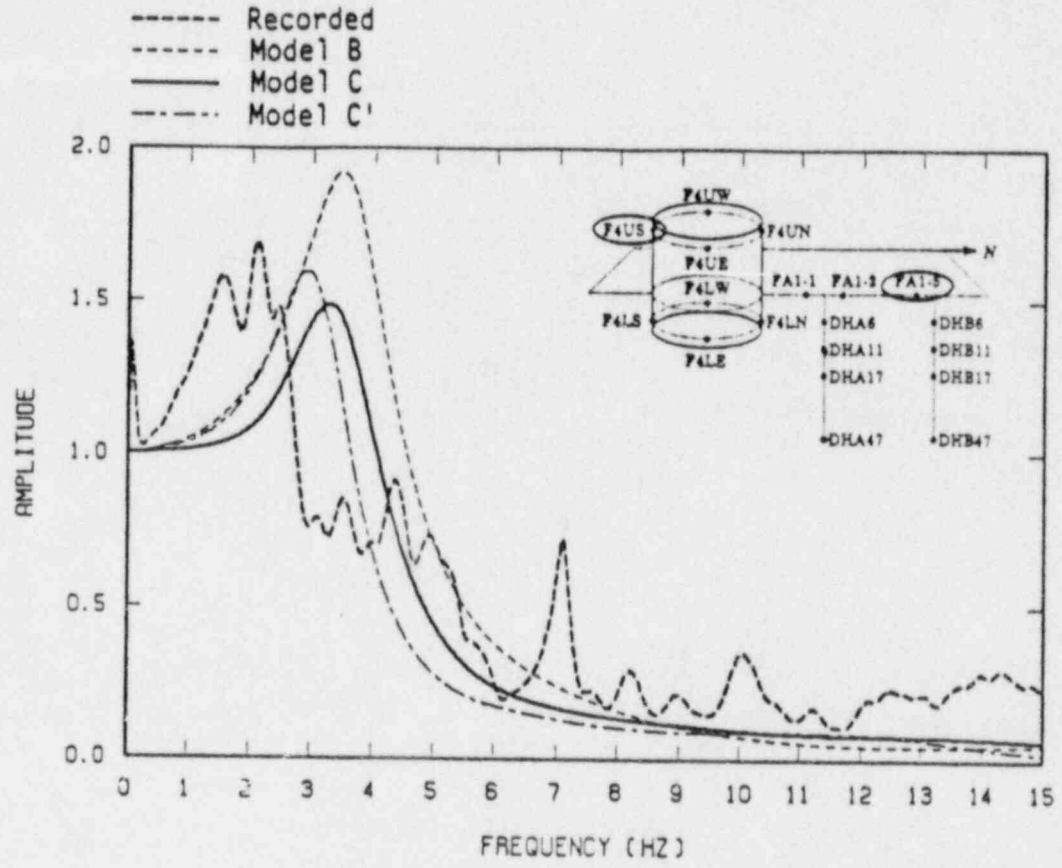

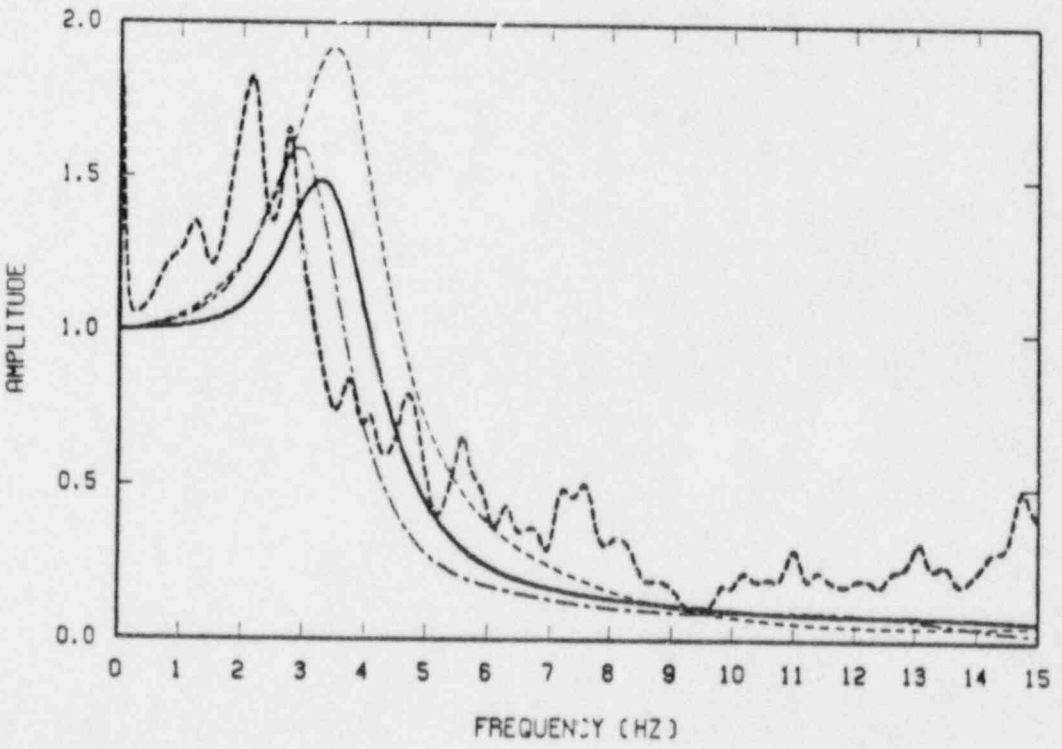

Figure 20. Transfer Functions for May 20, 1986 Earthquake (F4US-E/FA1-5-E)

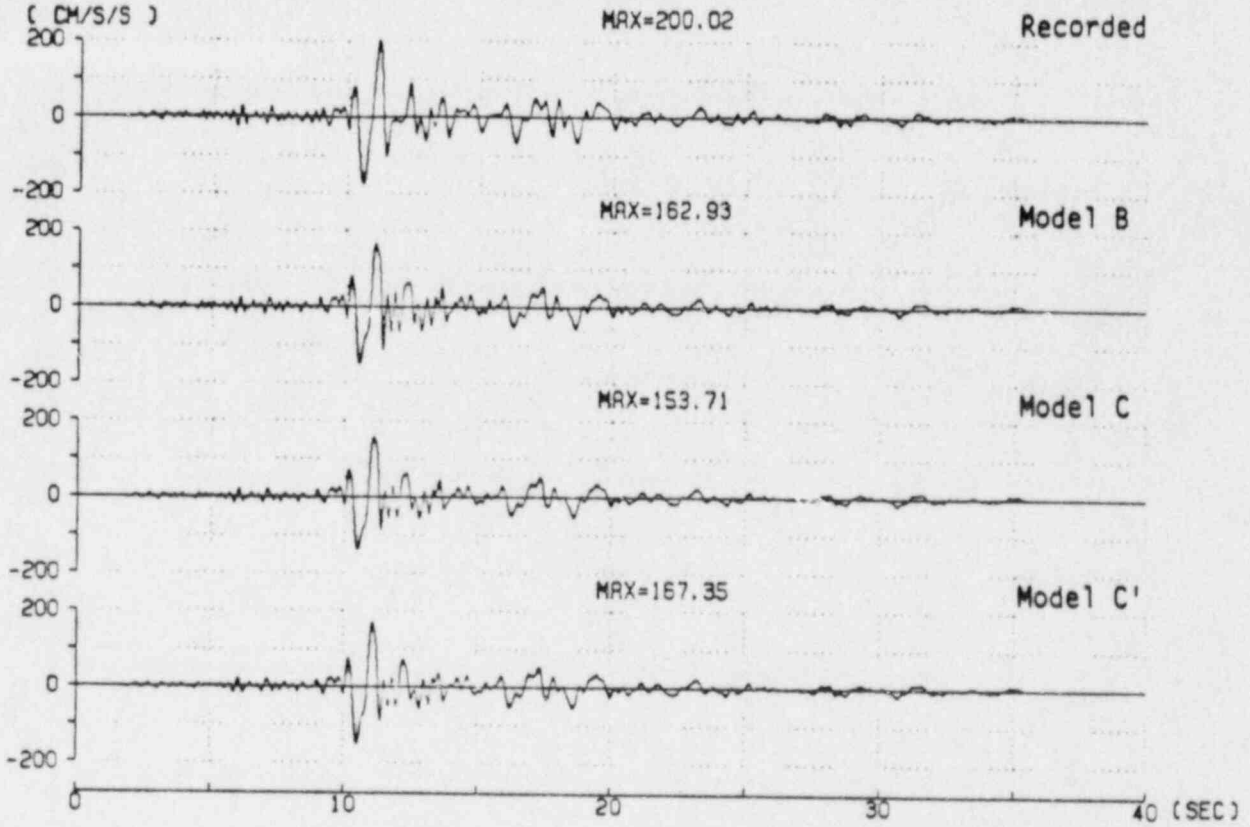

Figure 23. Acceleration Time Histories of F4US-E for May 20, 1986 Earthquake

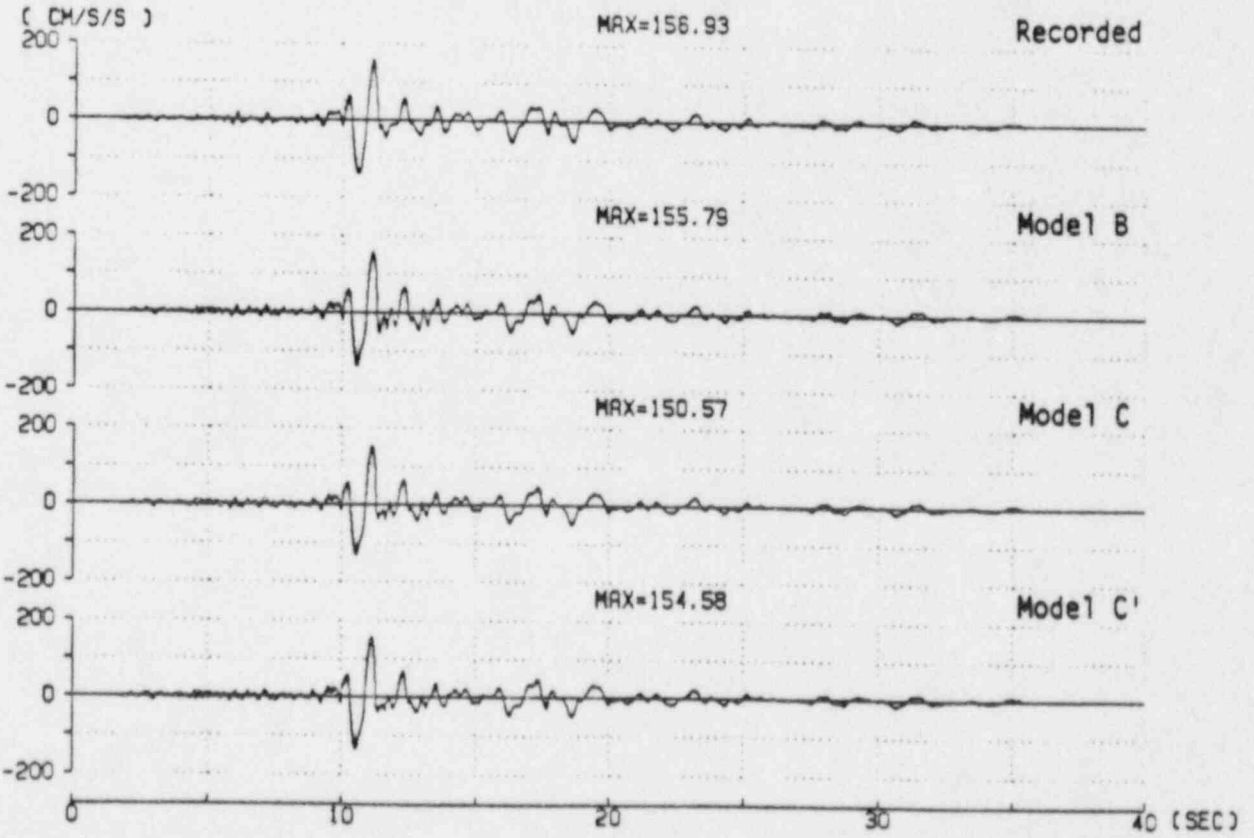

Figure 24. Acceleration Time Histories of FA1-1-E for May 20, 1986 Earthquake

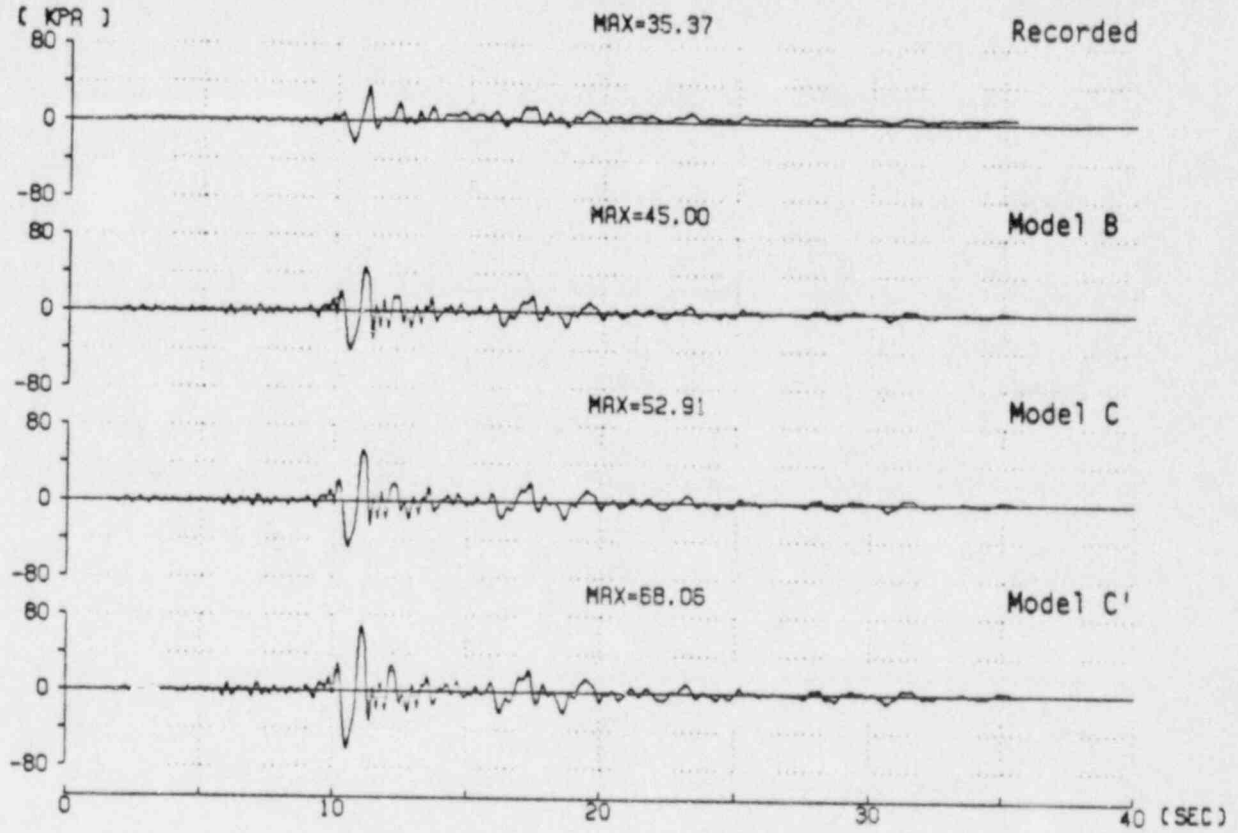

Figure 27. Pressure Time Histories of P4WS for May 20, 1986 Earthquake

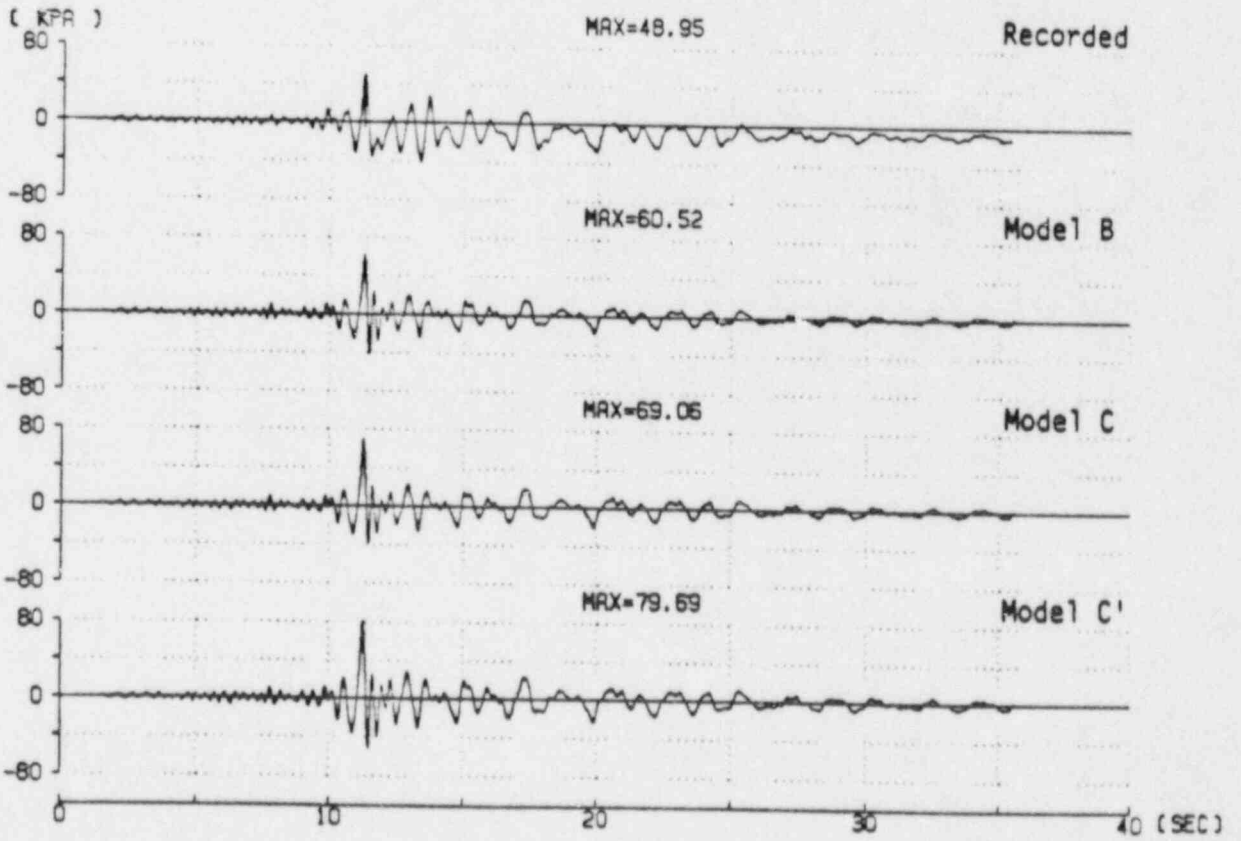

Figure 28. Pressure Time Histories of P4SW for May 20, 1986 Earthquake

RESPONSE PREDICTION AND RESULT COMPARISON FOR NOV. 14, 1986 EARTHQUAKE

The blind earthquake response analysis has also been carried out for the November 14, 1986 earthquake following the same procedure as for the May 20, 1986 earthquake. The refined model C' was utilized in this prediction. The maximum ground response and equivalent linear soil model obtained by SHAKE are shown in Fig. 29 and Table 8, respectively. The recorded maximum ground acceleration is also depicted in Fig. 29. A good agreement is seen between the predicted and recorded maximum ground acceleration.

Acceleration response spectra at DHB6 obtained by SHAKE and those at F4US, F4LS and FA1-1 obtained by AXERA are plotted in Fig. 30 to 33. Acceleration response spectra at DHB47 are not shown here since no record was available at this point. In these response spectra, a very good agreement is observed in the wide range of frequency. The transfer functions between the points, F4US and FA1-5, are plotted in Fig. 34 in the similar manner as for Fig. 20. The predicted transfer functions by the model C' excellently match those obtained from the actual records of November 14 earthquake. It is also observed that the system frequency by this November 14 event is almost the same as that by the May 20 event: f=1.8 to 2.5 Hz. Finally, acceleration time histories at F4US and FA1-1 are shown in Fig. 35 to 40, the pressure time histories at P4WS and P4SW are shown in Figs. 41 and 42, and the maximum acceleration and pressure values at the selected points are summarized in Table 9. In these figures and table, a good agreement between the prediction and observation is again confirmed except for the interface pressure. Hence the SSI model construction and modification procedure developed for May 20 earthquake may be valid for the other earthquakes of similar intensity.

From the comparison between the earthquake response analysis and recorded responses for the May 20 and the November 14 earthquakes, it may be concluded that the correlated model C' explain the response to the November 14 earthquake better than that to the May 20 earthquake. This is probably due to the fact that the recorded ground motions for the May 20 earthquake contain surface wave components, which are not considered in the current analysis, more than those for the November earthquake does.

Table 8

Equivalent Linear Soil Model for Nov. 14, 1986 Earthquake (Model C')

Layer No.	Depth G.L. (m)	Reduction Ratio G/G_0	V_s (m/s)	V_p (m/s)	Unit Weight γ_t (t/m^3)	Shear Modulus G (t/m^2)	Poisson's Ratio ν	Damping Ratio h
1	0.0 ▽ -5.0	0.55	63	262	1.87	760	0.469	0.100
2	▽ -8.0	0.55	104	810	1.87	2060	0.492	0.100
3	▽ -13.0	0.80	170	1270	1.87	5510	0.491	0.065
4	▽ -31.0	0.75	191	1330	1.87	6960	0.489	0.070
5	▽ -34.0	0.90	266	1330	1.90	13670	0.479	0.050
6	▽ -48.0	0.85	230	1250	1.90	10290	0.483	0.055
7	▽ -∞	0.85	249	1220	1.90	12000	0.478	0.055

Backfill (inner)	0.0 ▽ -5.0	0.35	62	323	2.24	878	0.481	0.105
Backfill (outer)	0.0 ▽ -5.0	0.70	88	323	2.24	1770	0.460	0.080

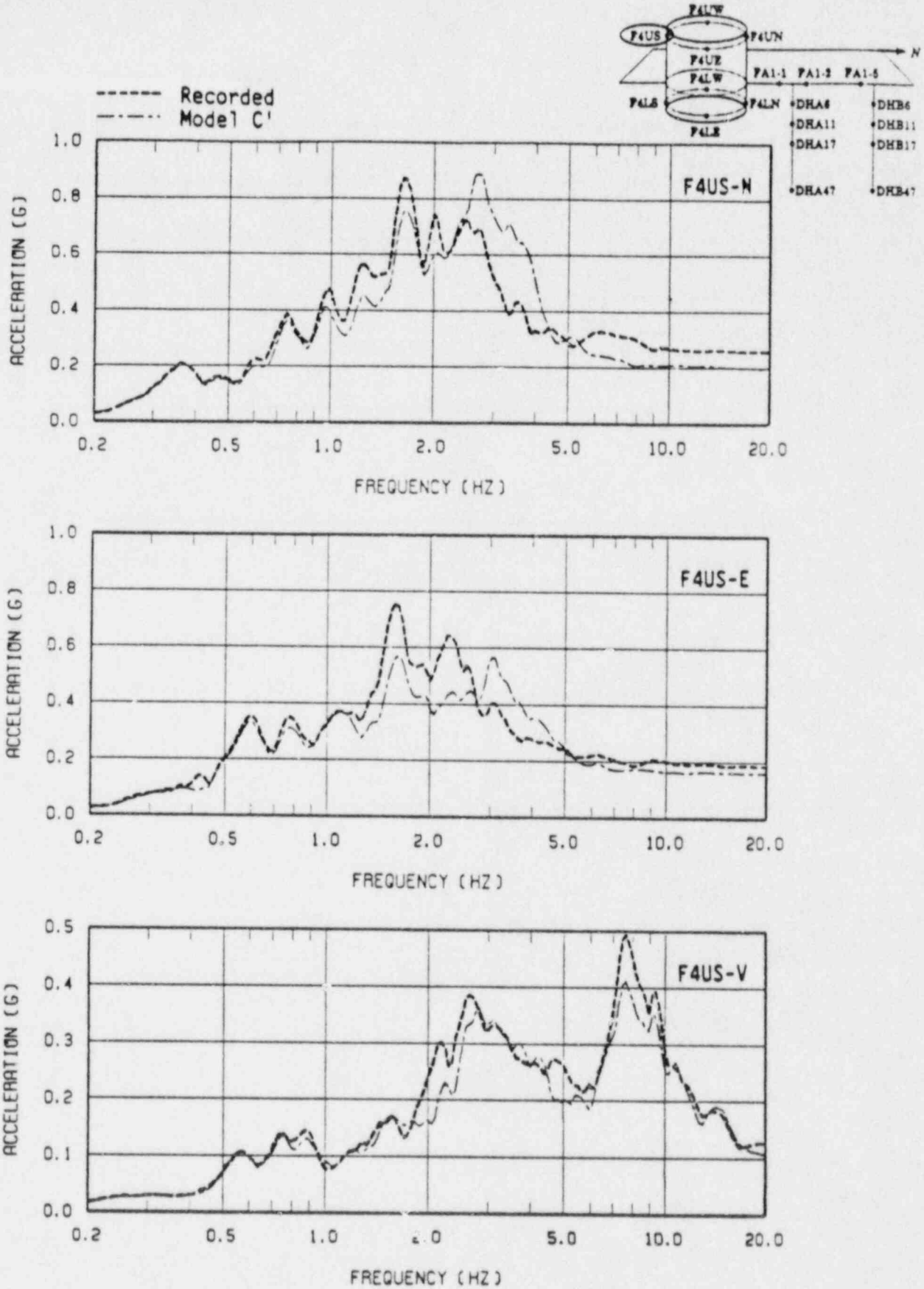

Figure 31. Acceleration Response Spectra at F4US for Nov. 14, 1986 Earthquake (h=5%)

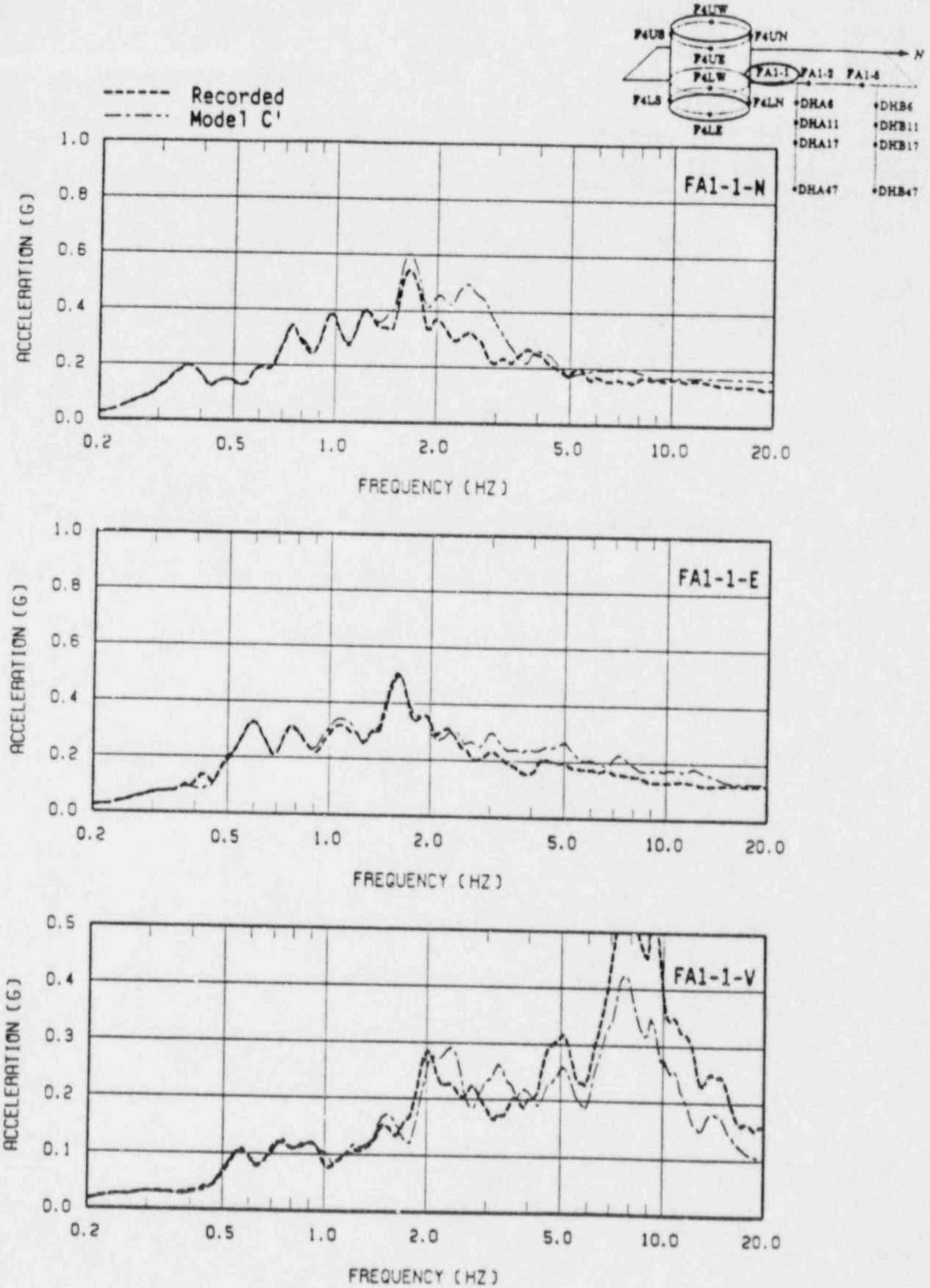

Figure 33. Acceleration Response Spectra at FA1-1 for Nov. 14, 1986 Earthquake (λ=5%)

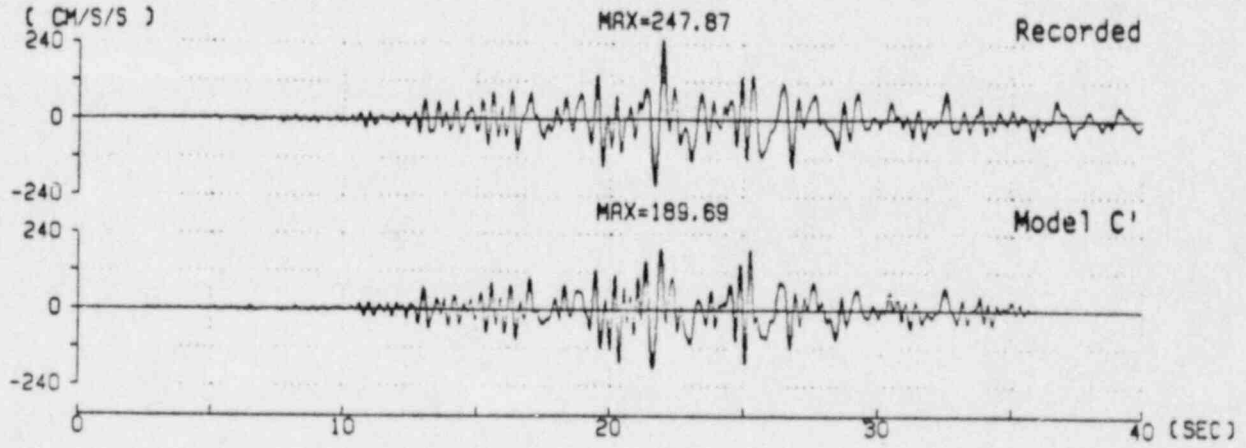

Figure 35. Acceleration Time Histories of F4US-N for Nov. 14, 1986 Earthquake

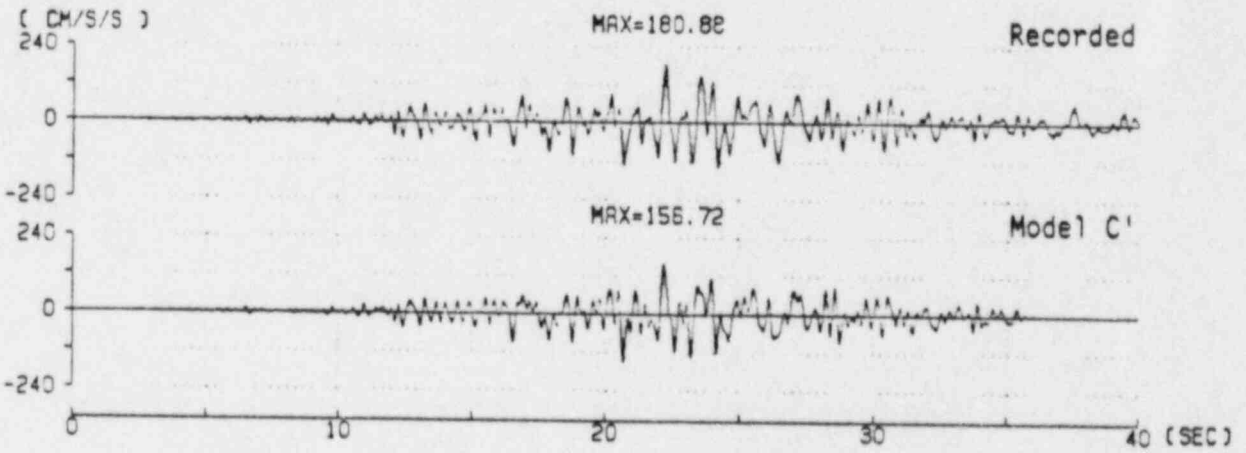

Figure 36. Acceleration Time Histories of F4US-E for Nov. 14, 1986 Earthquake

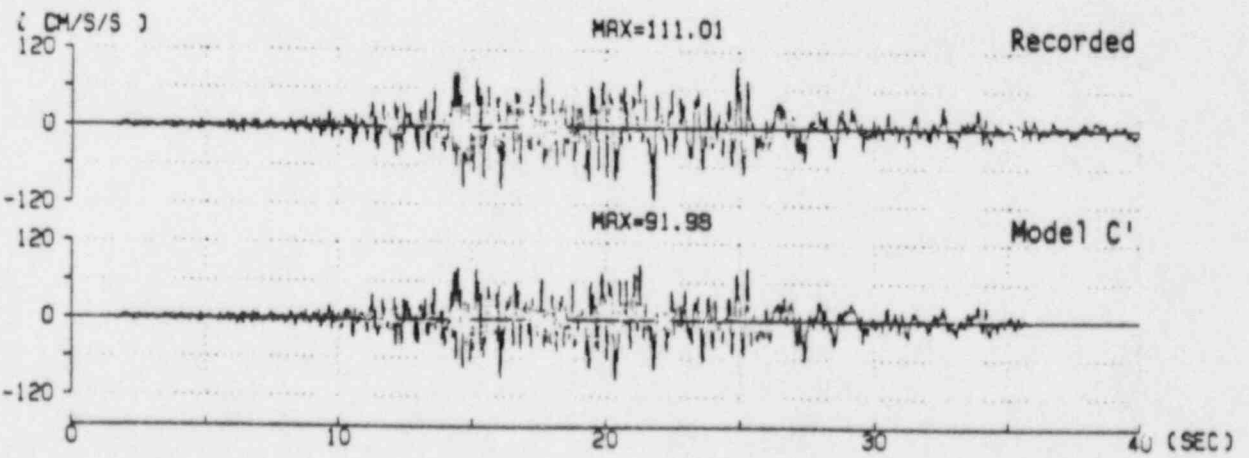

Figure 37. Acceleration Time Histories of F4US-V for Nov. 14, 1986 Earthquake

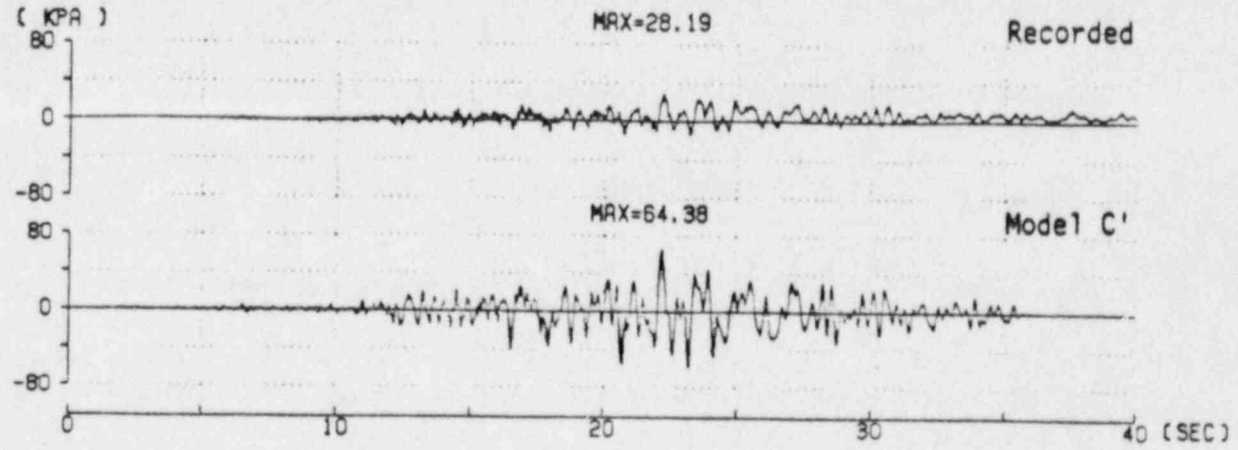

Figure 41. Pressure Time Histories of P4WS for Nov. 14, 1986 Earthquake

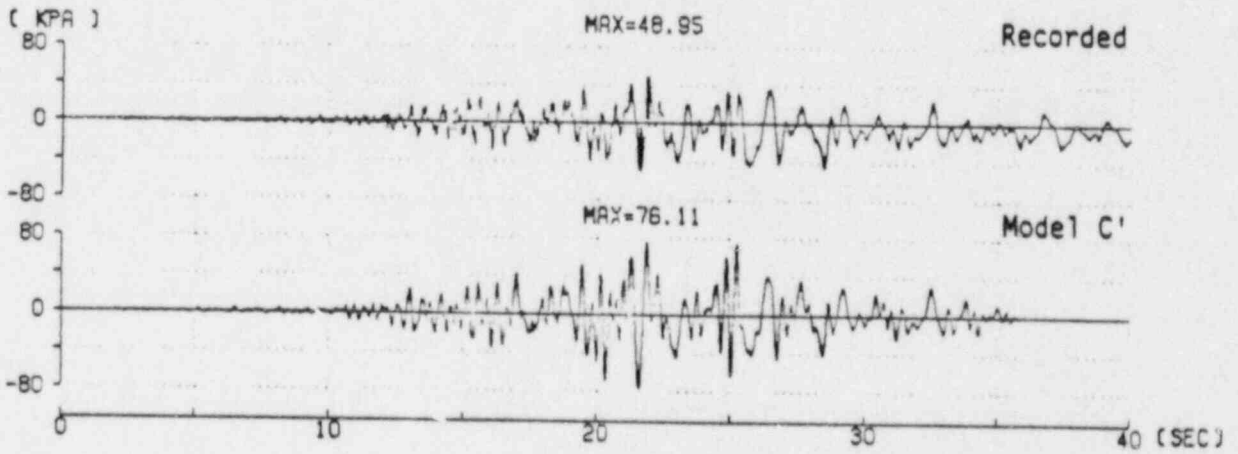

Figure 42. Pressure Time Histories of P4SW for Nov. 14, 1986 Earthquake

METHOD EVALUATION AND CONCLUSION

Forced Vibration Test (FVT)

The blind prediction analysis based on the data packages gave a good estimation for the system frequency and damping, and the mode shape of the response of the containment model to the forced vibration excitations. Hence the modeling of the soil and structure employed in this stage may be fairly close to the actual system. Although the elastic wave velocities of the backfill still remain unknown, the backfill might be harder than the top soil layer from the comparison between the analysis and measured results.

The realistic modeling capability of AXERA, i.e., viscoelastic layers with viscous dashpots on the bottom surface and the inhomgeneous soil region near the foundation, has also contributed to give the accurate estimates. The code AXERA is therefore considered to be able to simulate the soil-structure interaction system accurately when the soils are considered to be elastic media.

Earthquake Response

The equivalent linearization algorithm was employed in the deconvolution analysis for both May 20, 1986 and Nov. 14, 1986 earthquakes. The conventional value of effective strain factor α, 0.65 or 0.7, did not give convergence in the process to find strain compatible soil parameters. The shear strain induced in the upper soil layers during the earthquakes is considered to be large enough to exhibit the strong nonlinearity. When such large strain occurs, the deconvolution analysis based on the equivalent linearization algorithm may not be appropriate. It is also pointed out that frequency-independent complex damping ratios for soils may cause unrealistic increase of high frequency contents in ground responses when it is employed in deconvolution analyses of strong earthquakes.

A correlation analysis has been performed for the recorded ground motions of the May 20, 1986 and the November 14, 1986 earthquakes at FA1-5, FA2-5 and FA3-5. It showed that the horizontal phase velocity is very large, so that the assumption of the vertical incidence of the plane elastic waves may be reasonable. The estimated angle of incidence is less than 5° from the vertical axis at the top soil layer for the May 20 and the November 14 earthquakes.

In the equivalent linear algorithm, a careful attention should be paid for determining the equivalent damping ratio of soil. Although the conventional soil-structure analysis codes usually assume that the damping ratio associated with P-wave propagation is the same with that associated with S-wave propagation, it has been shown that such an assumption may reduce especially the vertical component of the response. Therefore it is suggested that the computer codes should be capable of defining different damping ratios for S- and P-waves, respectively.

The maximum pressures at P4WS and P4SW calculated using the model C' are somewhat

(2D)

SOIL-STRUCTURE INTERACTION ANALYSES OF QUARTER-SCALE CONTAINMENT MODEL EXPERIMENT IN LOTUNG, TAIWAN

Bechtel Group, Inc.
San Francisco, California

PREFACE

The work described in this paper was performed by Bechtel Power Corporation, San Francisco, under a contract agreement between Electric Power Research Institute (EPRI), Palo Alto, and Bechtel Group, Inc., San Francisco. The Bechtel project team for various phases of the project consisted of Bechtel engineers: Drs. W.S. Tseng, T. Takayanagi, S. Vahdani, K. Lilhanand, S.Y. Tuann, and F. Ostadan. W.S. Tseng was the principal investigator. A.H. Hadjian served as the project consultant.

PART 3: FLUSH METHOD

GENERAL DESCRIPTION OF THE FLUSH METHOD

Methodology and Computer Program

The FLUSH SSI analysis method is a two-dimensional (2-D) finite element soil-structure interaction analysis method using the frequency domain solution procedure. The computer program FLUSH was developed at the University of California, Berkeley (Ref. 3-1). The program has been widely applied in the U.S. nuclear industry for seismic SSI analysis of embedded structures. The version of FLUSH applied for this project is the public domain version which is available commercially at the CDC computer service bureau. This version of FLUSH has capabilities and limitations as summarized below:

- The soil medium of the SSI system must be horizontally layered soil strata overlaying a rigid base rock. No wave transmitting boundary is used at the rigid base boundary.

- The seismic input motion is assumed to be vertically propagating plane seismic S and P waves. The motion can be prescribed at any elevation within the free-field soil medium. The program can perform free-field deconvolution analysis of the input motion to generate the base boundary motion for the interaction analysis.

- The soil material is assumed to be linear viscoelastic material characterized by the complex moduli with constant hysteresis damping. The soil shear modulus and damping ratio can be specififed as functions of shear strain. The strain-dependent soil properties can be specified differently for every soil element in the SSI model.

- The program is a linear analysis program. However, it has the capability of automatically or manually performing a series of iterative, equivalent linear analyses to ensure strain compatibility of strain-dependent soil properties.

- The program has the options of specifying the horizontal wave transmitting boundary along either one or both side boundaries of the soil model and the viscous wave transmitting boundary at any point in the plane of the soil model to simulate 3-D wave radiation effect.

- The 2-D soil model is modelled with plane strain finite elements and the 2-D structural model can be modelled with 2-D beam elements. Special void elements can be used to simulate the basement void space of embedded structures.

Since the internal structures are located off the NS and EW axes of the containment, the structural model for the internal structures cannot be directly included in the 2-D FLUSH model. Thus it was decoupled from the containment model and not explicitly included in the 2-D FLUSH model. This decoupling is reasonable because of the relatively light internal structures. For determining the response of the internal structures, the containment base response motions at the internal structure support location were obtained from the 2-D FLUSH SSI analyses. These motions were properly combined to give the 3-component base motions which were then, applied as the base input motions for 3-D fixed-base response analyses for the internal structures. For these decoupled analyses, the 3-D lumped-mass stick models of Model B and Model C for the internal structures described in Part 1 were directly used. Thus, the difference between Model B and Model C for FLUSH analyses was only in the internal structure models.

FLUSH Model

The configuration of the FLUSH SSI model developed is shown in Fig. 3-2. The model is a half model with anti-symmetric boundary condition at the centerline for the horizontal NS and EW analyses, and with symmetric boundary condition for the vertical analyses. The model consists of 2-D lumped-mass beam stick model for the containment and 2-D plane strain finite elements for the soil medium. The depth of soil medium included in the FLUSH model above rigid base was chosen from the result of a sensitivity study in which the depth of the soil model was varied and the sensitivity of the containment response was evaluated.

The finite element mesh of the FLUSH model was sized to pass seismic S and P waves up to a maximum frequency of 10 cps. The horizontal wave transmitting boundary was used for the right-hand side boundary of the model. The viscous wave transmitting boundary was applied to every soil node in the model.

Since the 2-D containment stick model is the same for the NS and EW directions, the FLUSH model shown in Fig. 3-2 is applicable for both the horizontal NS and EW analyses. The initial low-strain soil profile used for the FLUSH model was the best-estimate low-strain soil properties as given in Tables 1-1 and 1-2 of Part 1.

EARTHQUAKE RESPONSE PREDICTIONS AND RESULT COMPARISONS

Earthquake response predictions have been made using the FLUSH computer program for both earthquake events, LSST07 dated 5/20/86 and LSST16 dated 11/14/86. The response predictions for the internal structures have been made for both earthquake events using both Model B and Model C internal structure models.

The input motions to the FLUSH analyses were the free-field surface recorded motions at the recording station FA1-5. These motions were assumed to be prescribed at the surface of the FLUSH soil model. FLUSH free-field deconvolution analyses were performed to obtain the strain-compatible soil properties and the free-field soil response motions at the free-field downhole recording station DHB6 which is located at 6 m below grade. The free-field soil response motions at DHB47, located 47 m below grade, were not calculated since the FLUSH model did not extend to this depth. The strain-compatible soil properties as obtained were very similar to those obtained from SHAKE analyses presented in Figs. 1-15 of Part 1.

response amplitudes agree well with the corresponding recorded amplitudes. The decoupled internal structure response provides acceptable results due to its relative small mass.

From the result of this study, it may be concluded that the FLUSH method of SSI analysis with the associated model parameters applied in this project, in particular the modeling of the equivalent strip, is adequate but slightly on the unconservative side. This may be caused partly by the criteria for developing the equivalent strip and partly by the viscous dampers used for simulation of 3-D wave radiation which may have over estimated the damping for the FLUSH soil model.

REFERENCES

3-1. Lysmer, J., Udaka, T., Tasi, C. F., and Seed, H. B., "FLUSH - A Computer Program for Approximate 3-D Analysis of Soil-Structure Interaction Problems," Report No. EERC-75-30, University of California, Berkeley, 1975.

3-2. Hadjian, A. H., Luco, J. E., and Wong, H. L., "On the Reduction of the Three-Dimensional Analysis of Soil-Structure Interaction Problems to Two-Dimensional Models," Proceedings of the 2nd ASCE/EM Specialty Conference on the Dynamic Response of Structures, Atlanta, Georgia, January 1981.

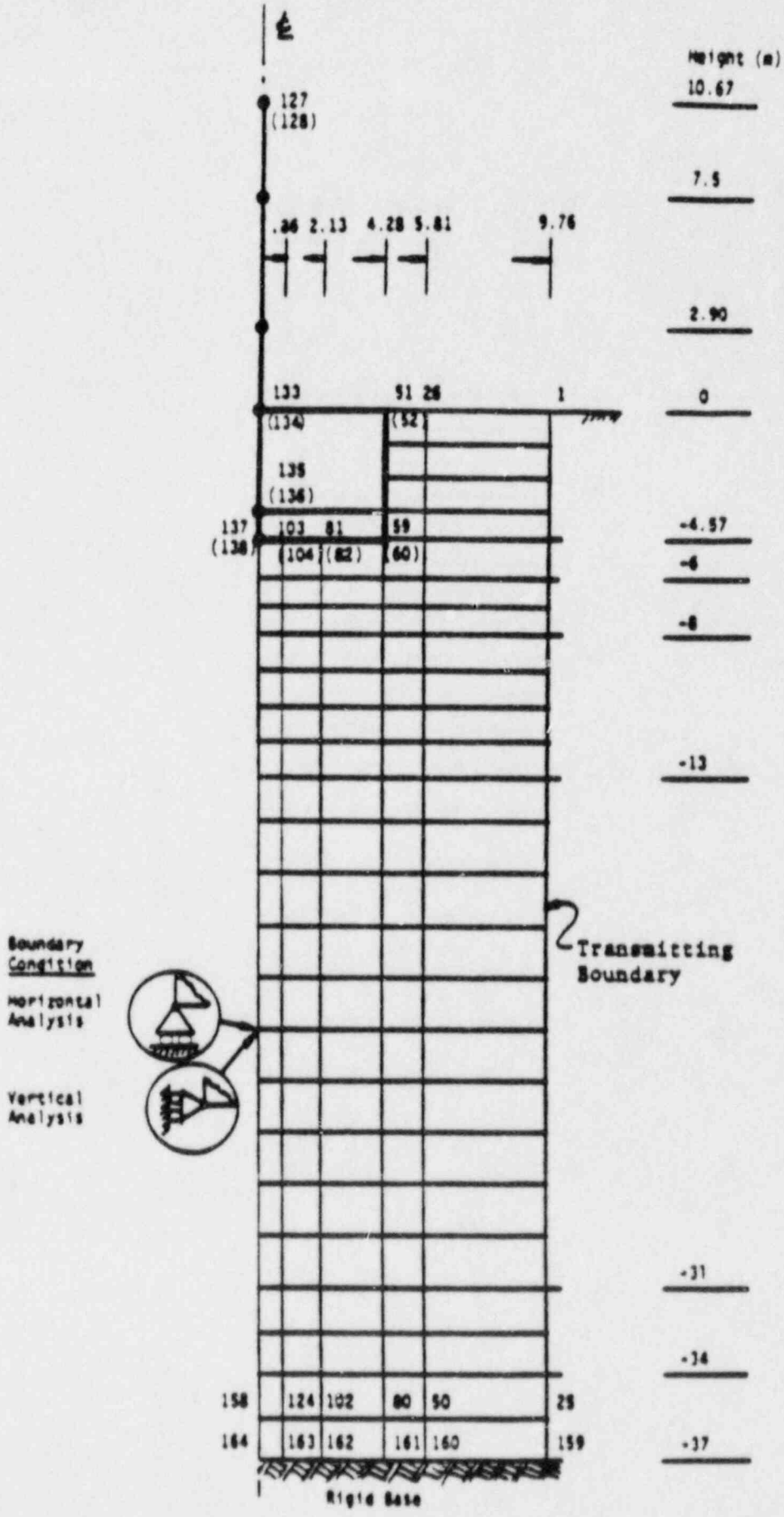

Figure 3-2. Configuration of FLUSH 2-D Finite Element Models B & C

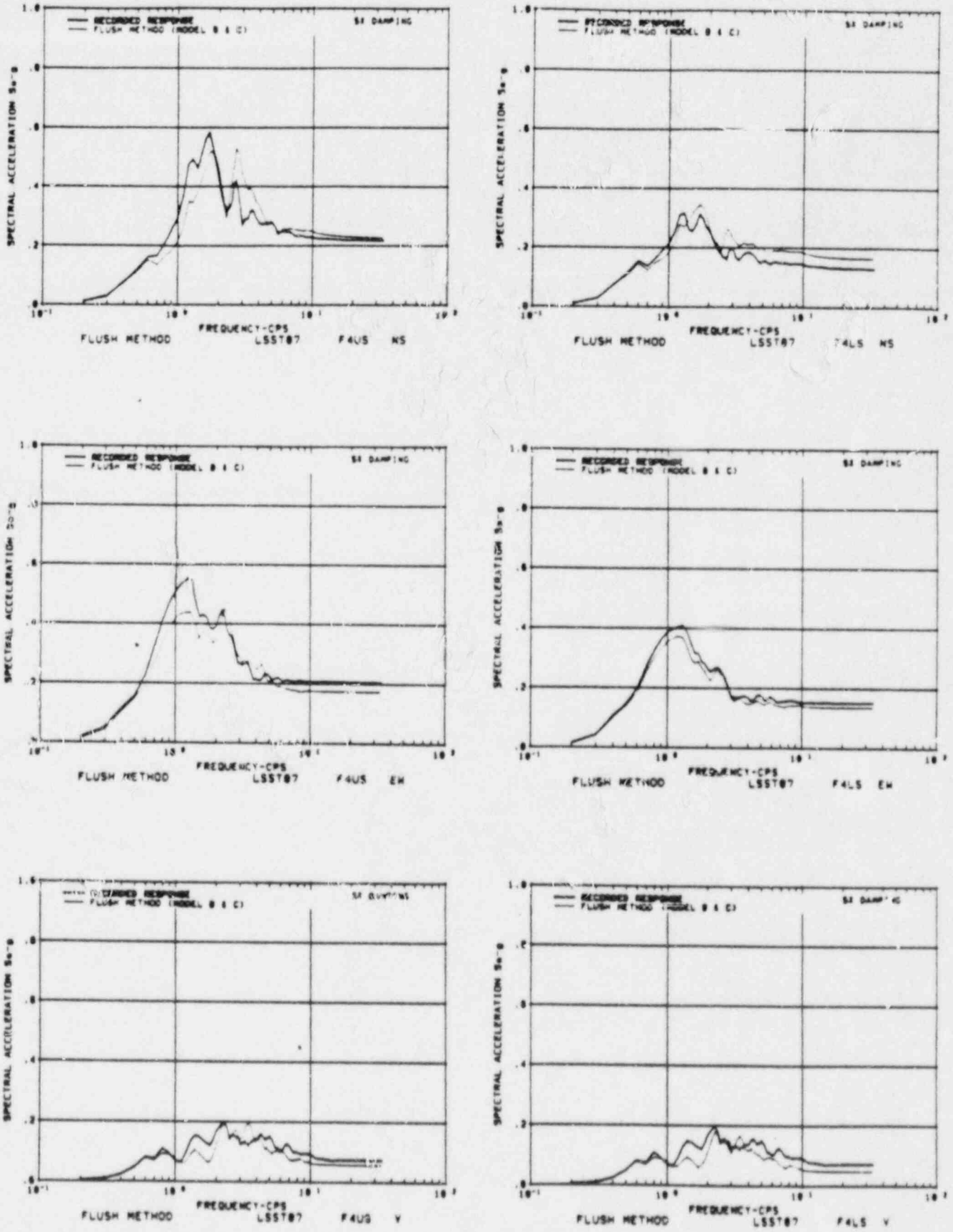

Figure 3-4. Response Spectra at F4US and F4LS for Models B & C (LSST07 Surface Input)

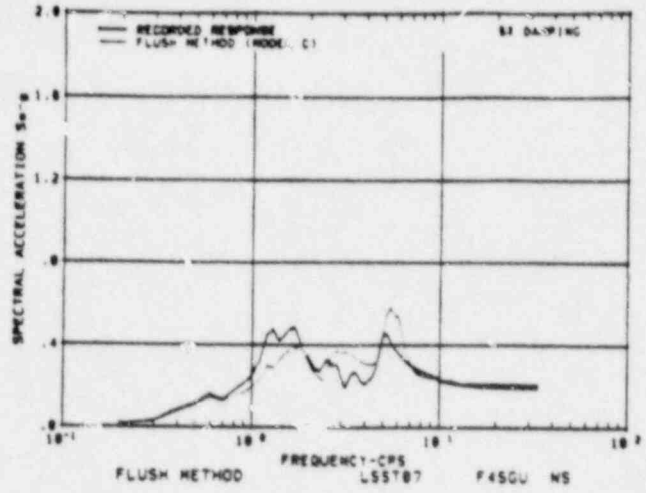

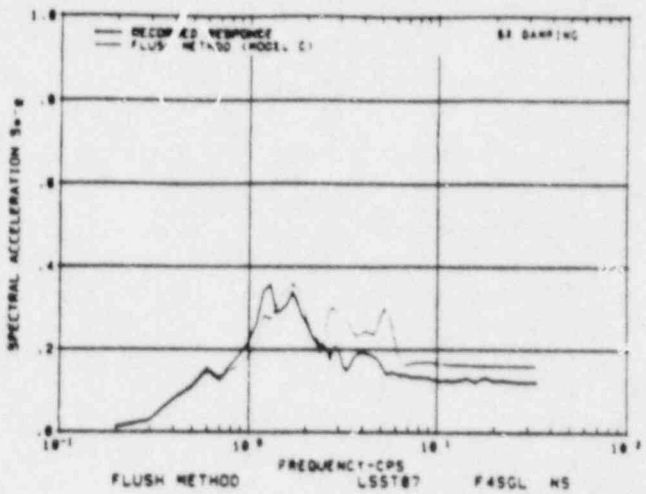

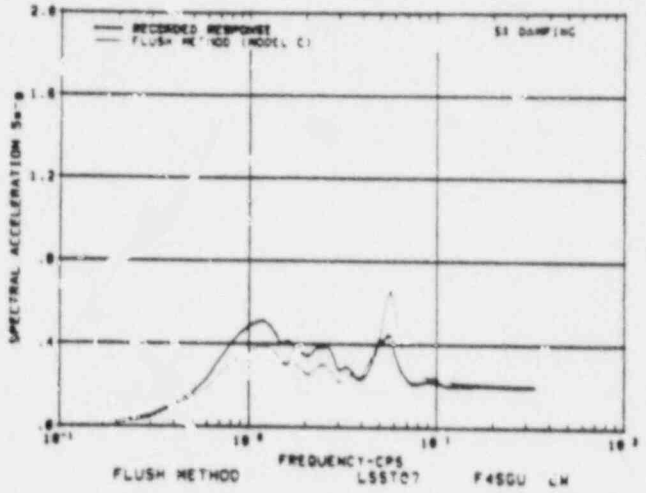

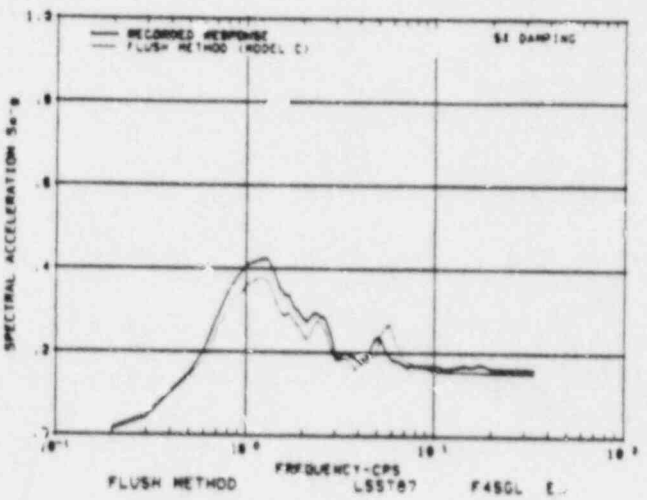

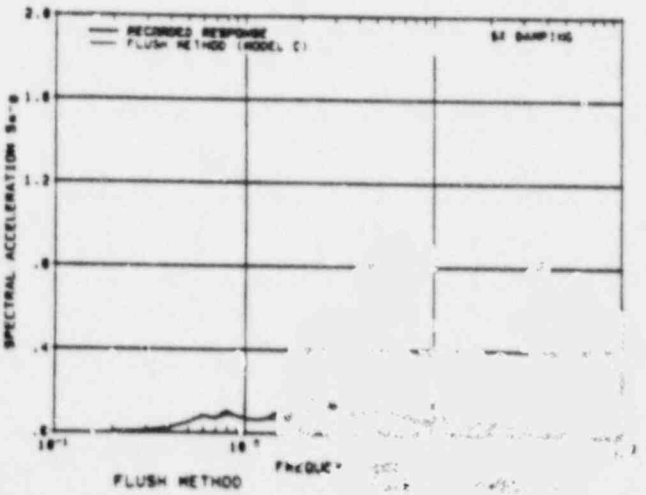

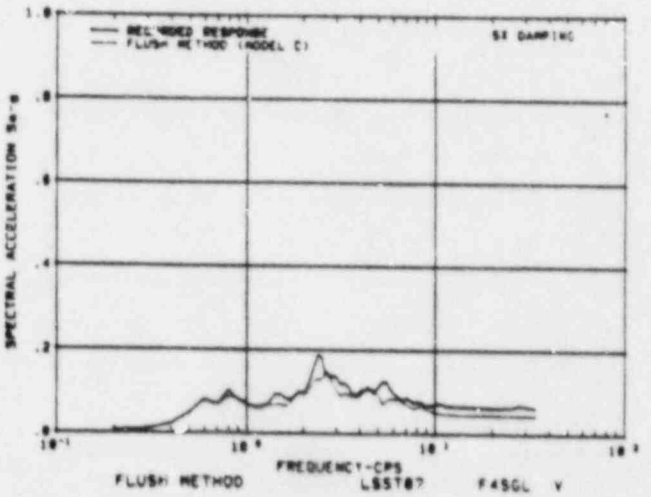

Figure 3-6 Response Spectra at F4SGU and F4SGL for Model C (LSST07 Surface Input)

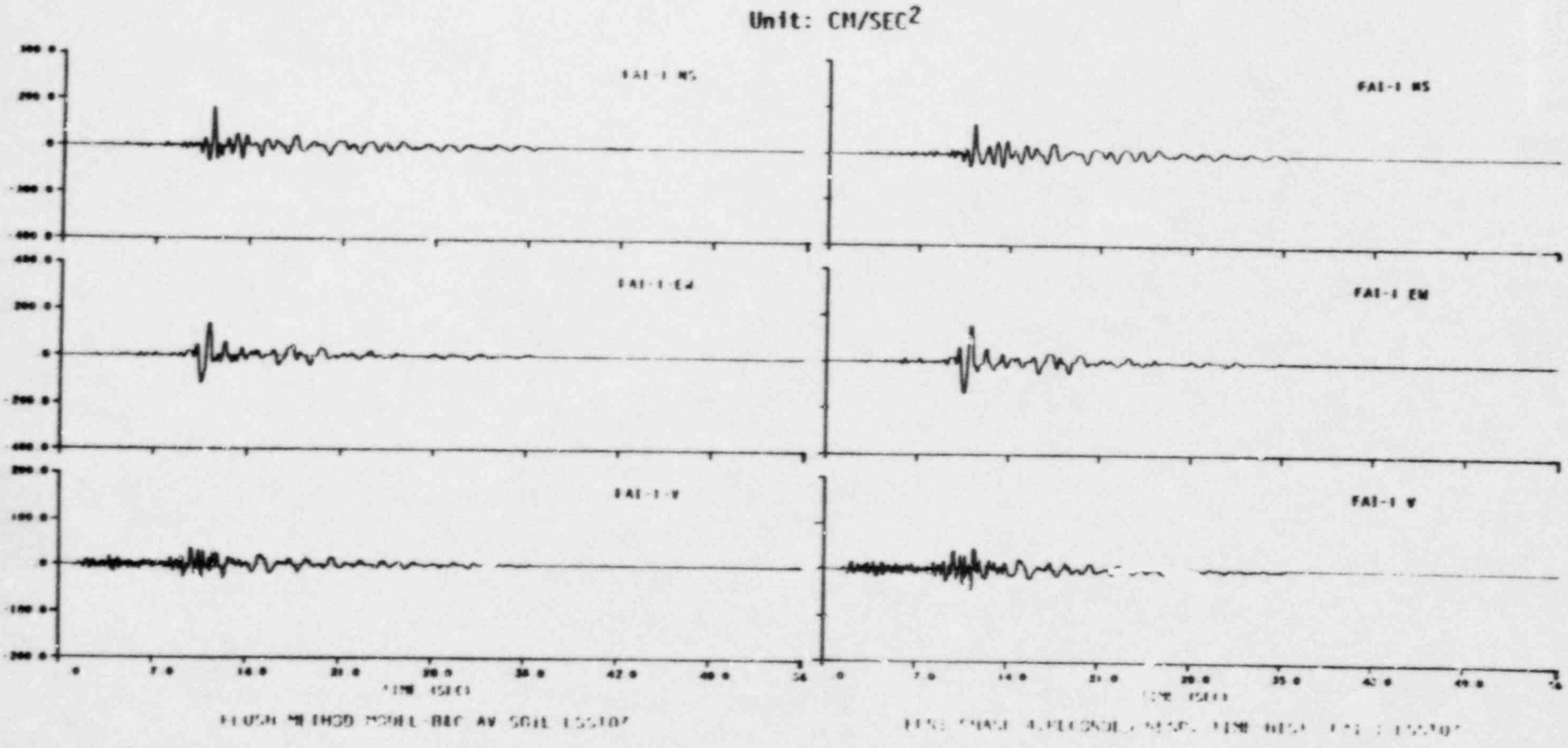

Figure 3-8. Response Acceleration Time Histories at FAI-1 for Models B & C (LSST07 Surface Input)

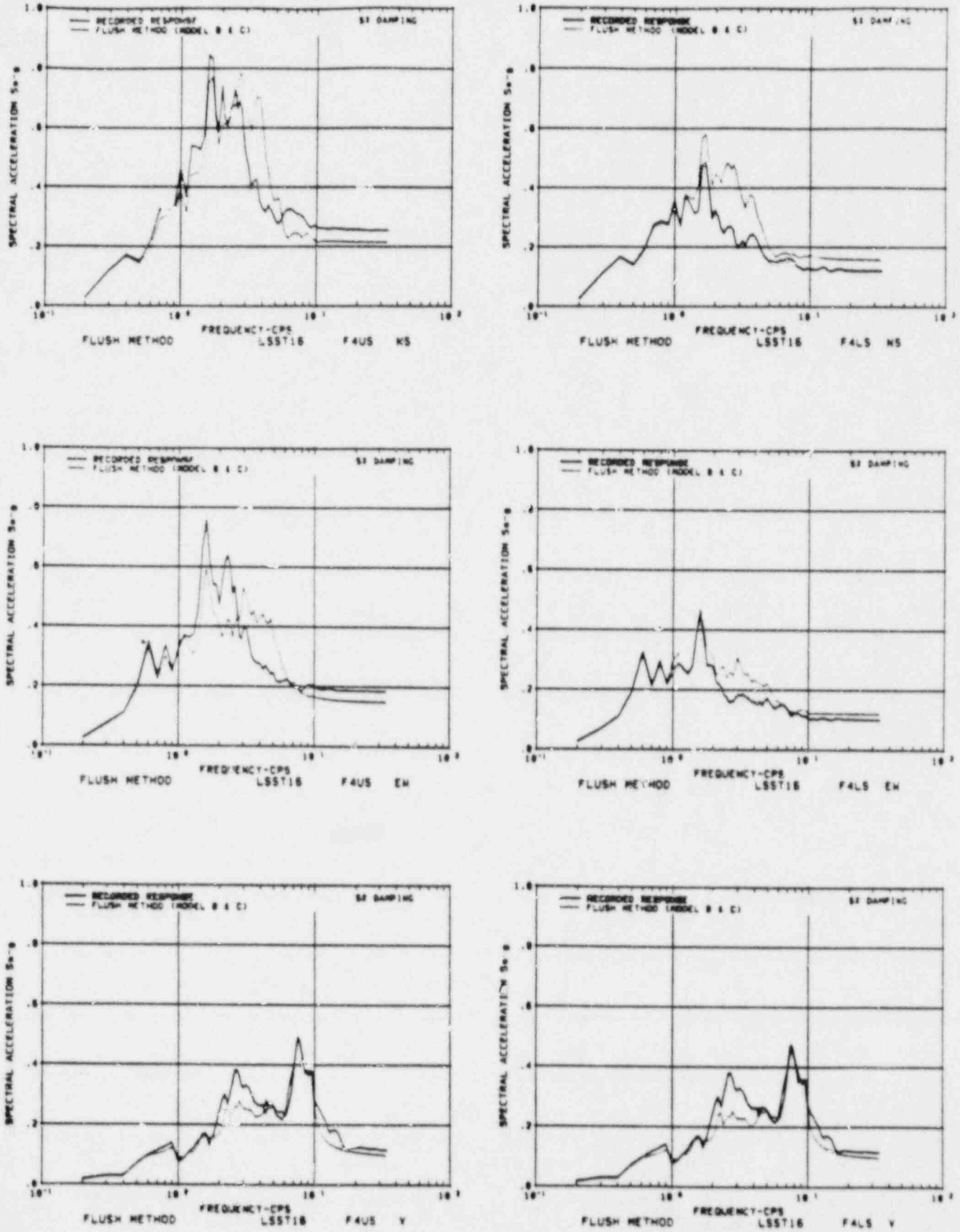

Figure 3-10. Response Spectra at F4US and F4LS for Models B & C (LSST16 Surface Input)

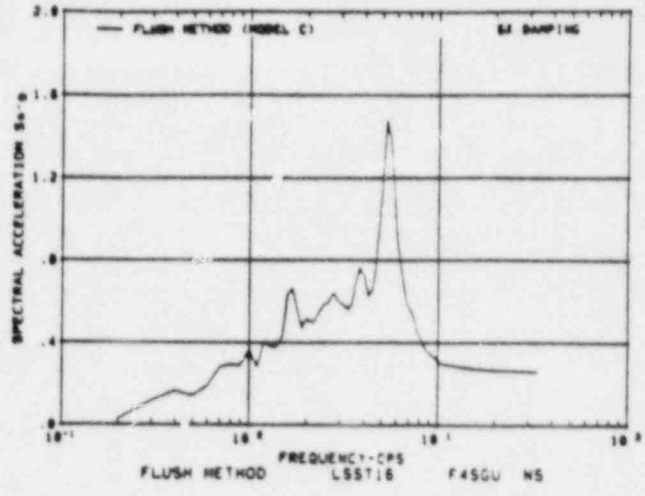

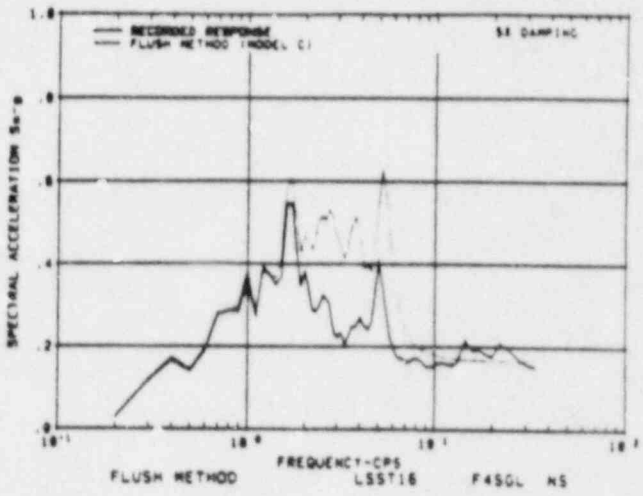

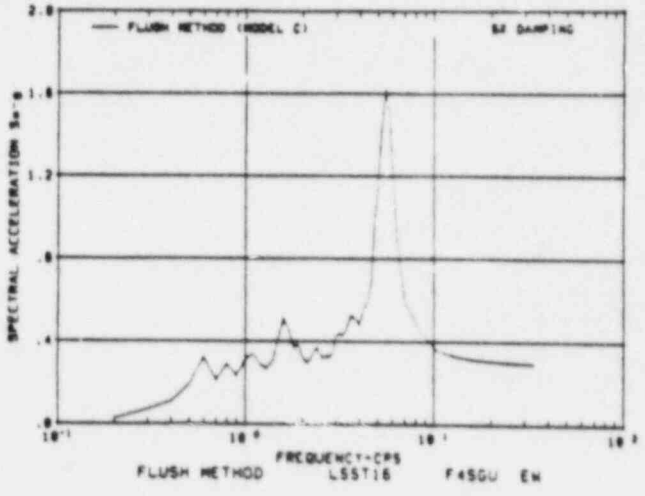

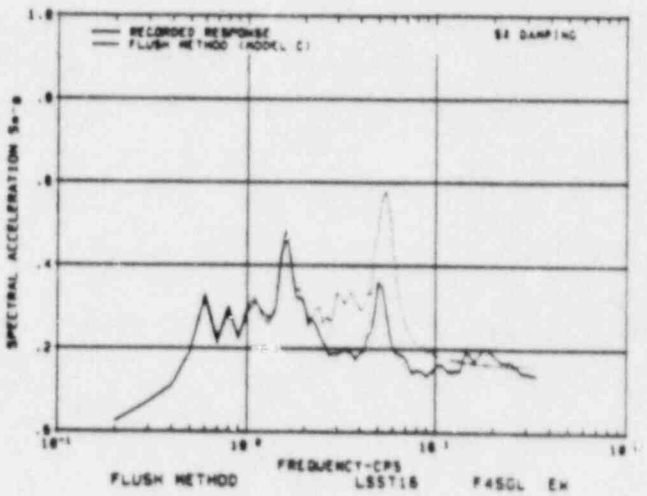

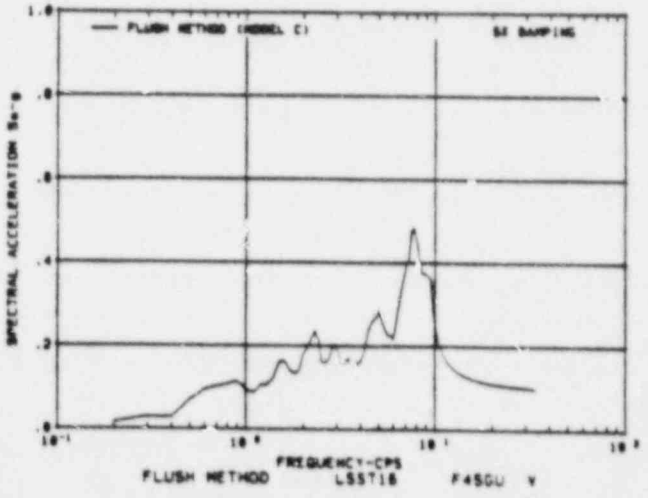

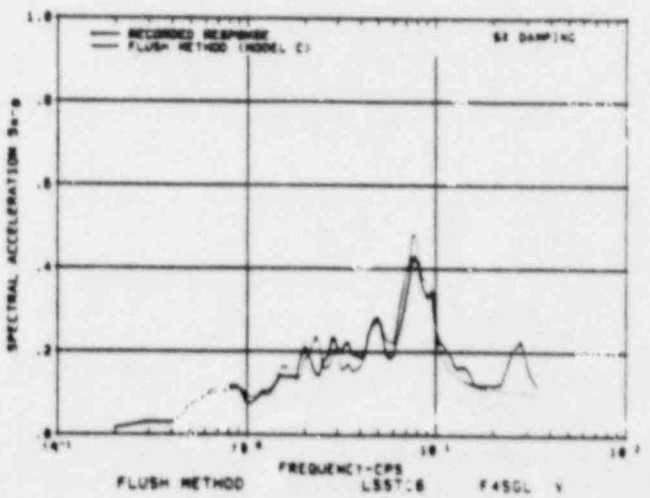

Figure 3-12. Response Spectra at F4SGU and F4SGL for Model C (LSST16 Surface Input)

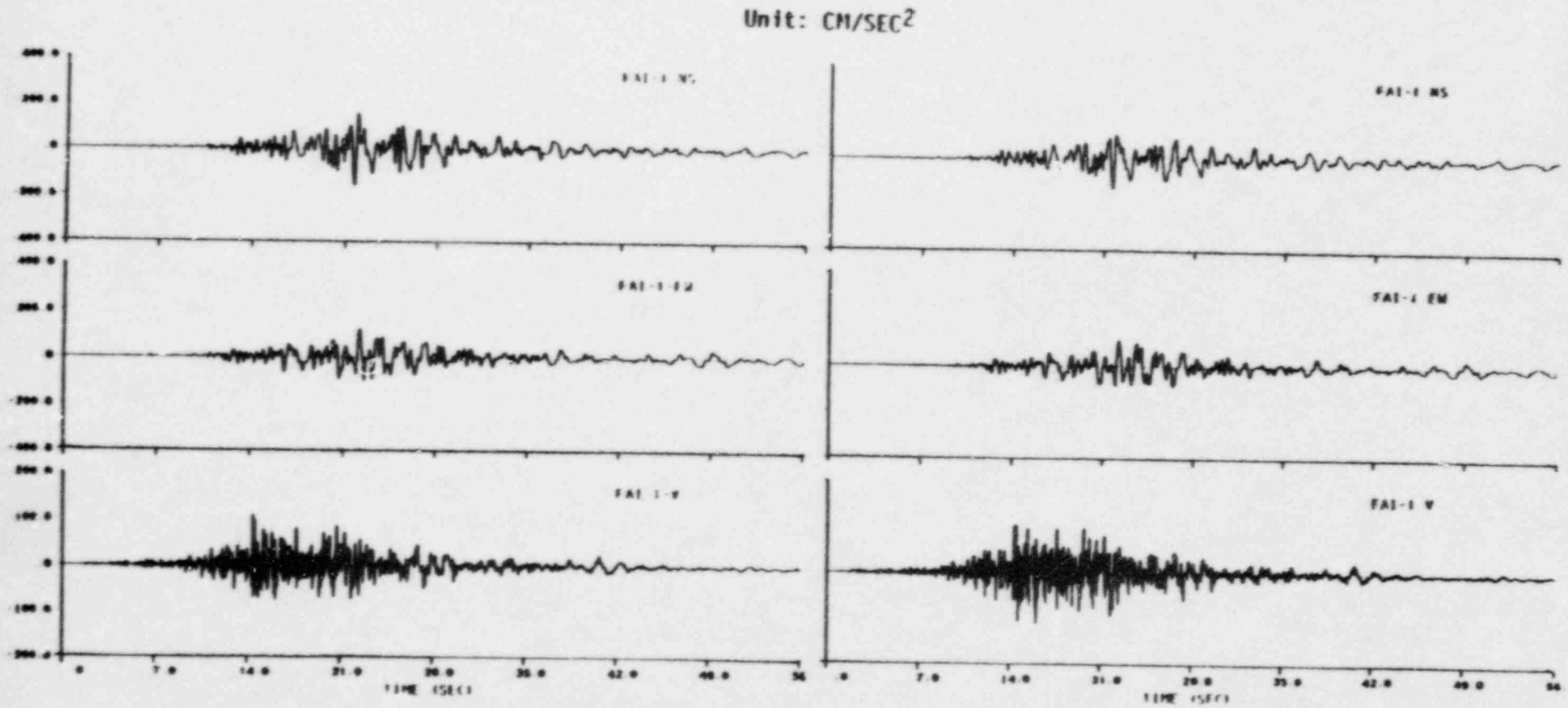

Figure 3-14. Response Acceleration Time Histories at FA1-1 for Models B & C (LSST16 Surface Input)

COMPUTATIONAL PARAMETERS AND THEIR LIMITATIONS

Introduction

The following paragraphs describe the enveloping, broadening, and smoothing procedures that have been followed to obtain final floor response spectra (FRS) for Oyster Creek project. This is in response to item 3 of NRC memo (Ref. Memo from Mr. A. Dromerick (NRC) to Mr. P. B. Fiedler (GPU), dated December 16, 1987).

Enveloping Procedure

Seismic responses for the Oyster Creek reactor building were obtained by three soil-structure interaction (SSI) analyses assuming three different soil profiles -- best estimate, upper bound, and lower bound. Raw floor acceleration response spectra were computed from each of the three analyses. The three raw spectra at each selected location were then enveloped to obtain the final raw spectra. Figure 1 shows the three raw horizontal spectra at the basemat level (elevation -19'-6") in the reactor building. Figure 2 presents the enveloped raw spectra.

Broadening/Smoothing Procedure

The spectral peaks of the enveloped raw spectra were broadened ±15% at fixed-base structural frequencies following USNRC Reg Guide 1.122. This broadening was done to account for any variations in structural frequencies due to any possible uncertainties in building structural properties. The soil-structure peaks were enveloped and not broadened, since variations in soil properties were accounted for in the analysis by considering the best estimate, upper bound, and lower bound soil shear modulus cases. Figure 3 presents the broadened/smooth horizontal spectra at basemat elevation.

For the purposes of peak broadening, the fixed base structural frequencies were obtained from the eigenvalue analysis of the model. Table 1 presents the frequencies for the reactor building model. The lowest horizontal frequency, for example, is 5.4 Hz (0.184 sec). In our broadening procedure, all the structural peaks at this frequency or at higher frequencies were

broadened ±15%. Peaks at lower frequencies are primarily due to soil effects and were enveloped from the three soil profile cases.

Figures 4, 5, and 6 present individual raw, enveloped raw, and smooth/broadened final vertical spectra at a typical slab location (elevation 51'-3") in the reactor building.

Conclusion

The enveloping, peak broadening, and smoothing procedures, adopted for obtaining the final floor response spectra (FRS) for Oyster Creek reactor building, have rigorously accounted for any peak variations in the FRS that may occur due to possible variations in the soil and structure properties used in the analyses. Soil property variations are considered by enveloping results from three sets of soil properties. Structural property variations are accounted for by broadening structural peaks by ±15%.

TABLE 1

FREQUENCIES AND MODAL PARTICIPATION FACTORS

FOR THE FIXED-BASE REACTOR BUILDING MODEL

Mode No.	Freq. (CPS)	Period (Sec)	Modal Partic. Factors		
			X-Dir.	Y-Dir.	Z-Dir.
1	5.42	0.184	33.6	-0.4	-2.0
2	5.45	0.183	0.0	-0.5	31.8
3	6.22	0.161	27.1	-0.5	-8.1
4	6.27	0.159	-8.4	0.9	-27.9
5	7.32	0.136	-0.0	0.0	0.0
6	8.05	0.124	17.6	0.2	0.8
7	8.11	0.123	0.1	0.3	-17.9
8	9.47	0.106	-3.1	-0.1	8.2
9	12.52	0.080	0.0	0.4	0.0
10	14.39	0.069	-2.8	-1.7	-6.4
11	14.40	0.069	-6.2	-1.1	2.7
12	14.82	0.067	0.2	-0.0	-0.8
13	15.41	0.065	-0.0	-0.0	-0.0
14	15.58	0.064	2.9	48.7	2.2
15	18.46	0.054	1.8	-4.8	1.6
16	18.64	0.054	3.1	-0.7	-0.0
17	18.71	0.053	-0.1	-0.6	6.1
18	19.90	0.050	-0.0	-3.1	22.1
19	20.63	0.048	-21.8	5.7	0.1
20	23.06	0.043	1.3	-0.5	-0.0
21	23.06	0.043	0.0	-0.2	1.5
22	25.51	0.039	-3.5	-0.6	-0.9
23	28.82	0.035	-15.0	-1.2	3.3
24	28.97	0.035	3.2	1.8	13.7
25	29.66	0.034	-1.2	-0.1	-0.0
26	29.67	0.034	0.4	0.0	0.2
27	31.12	0.032	8.3	0.3	-1.2
28	31.23	0.032	1.6	2.3	7.8
29	32.09	0.031	0.6	7.3	-2.8
30	36.90	0.027	-0.3	7.5	-0.2

X = North-south direction
Z = East-west direction
Y = Vertical direction

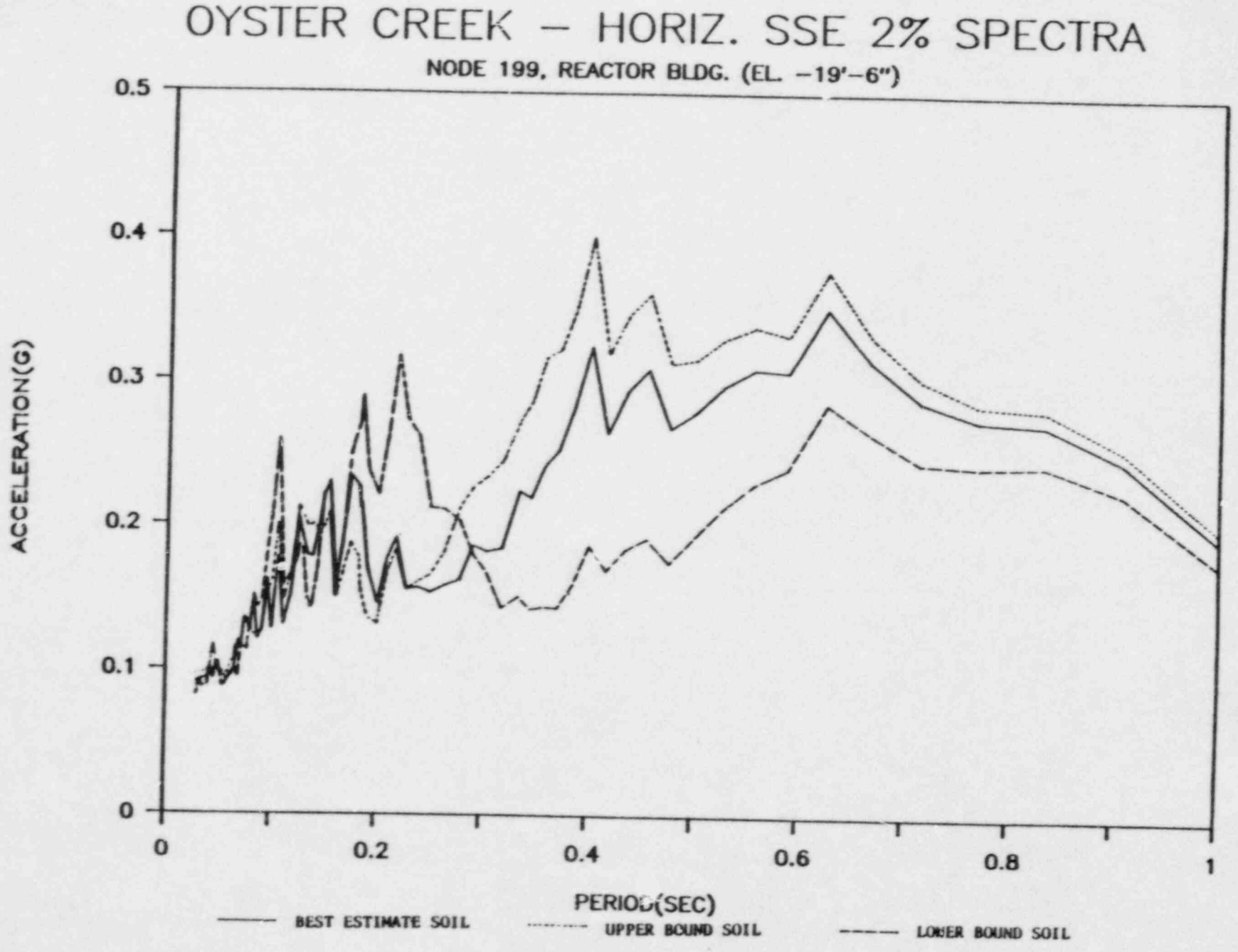

FIGURE 1 RAW HORIZONTAL SSE SPECTRA AT BASEMAT LEVEL OF THE REACTOR BUILDING

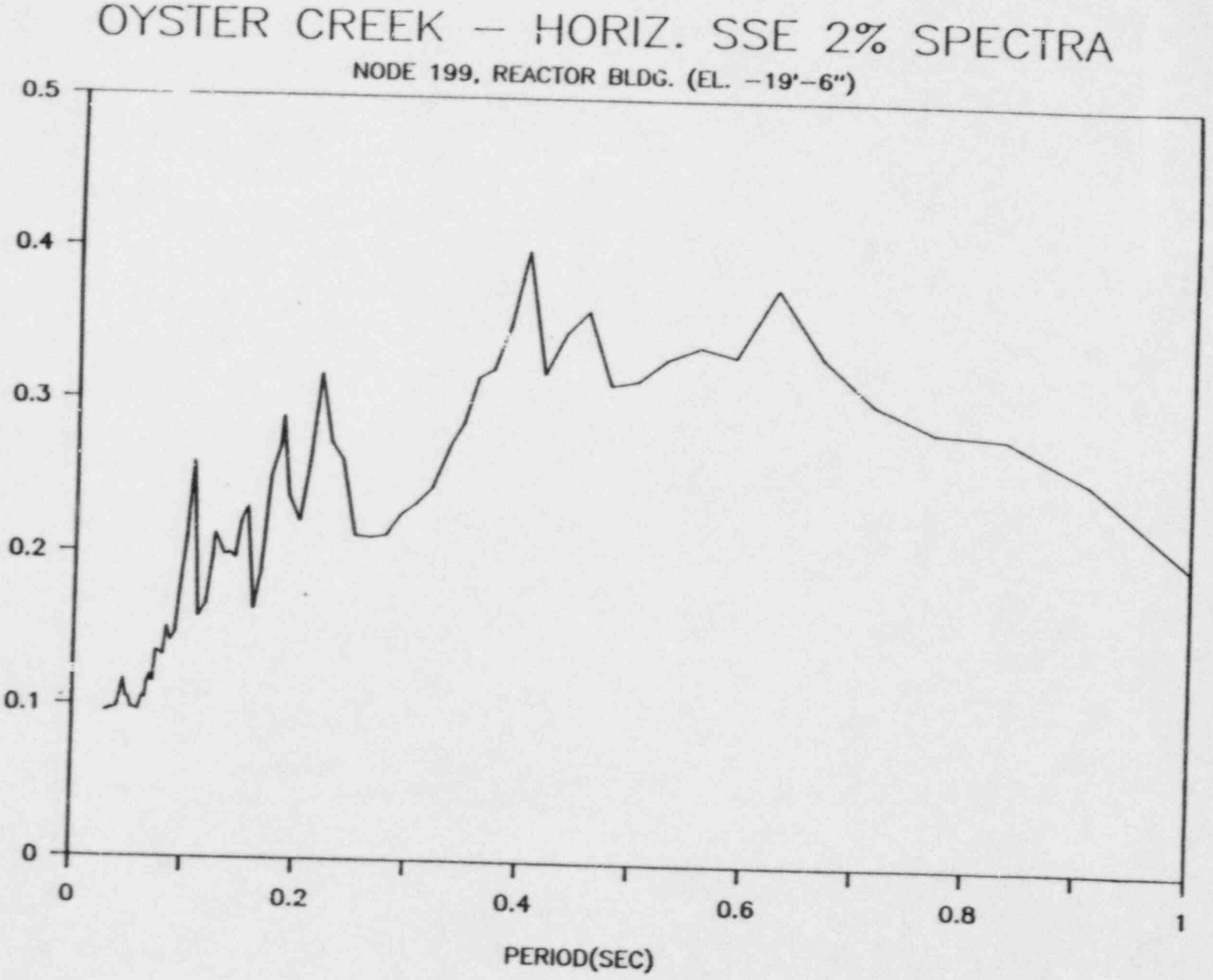

FIGURE 2 RAW ENVELOPED HORIZONTAL SSE SPECTRUM AT BASEMAT LEVEL OF THE REACTOR BUILDING

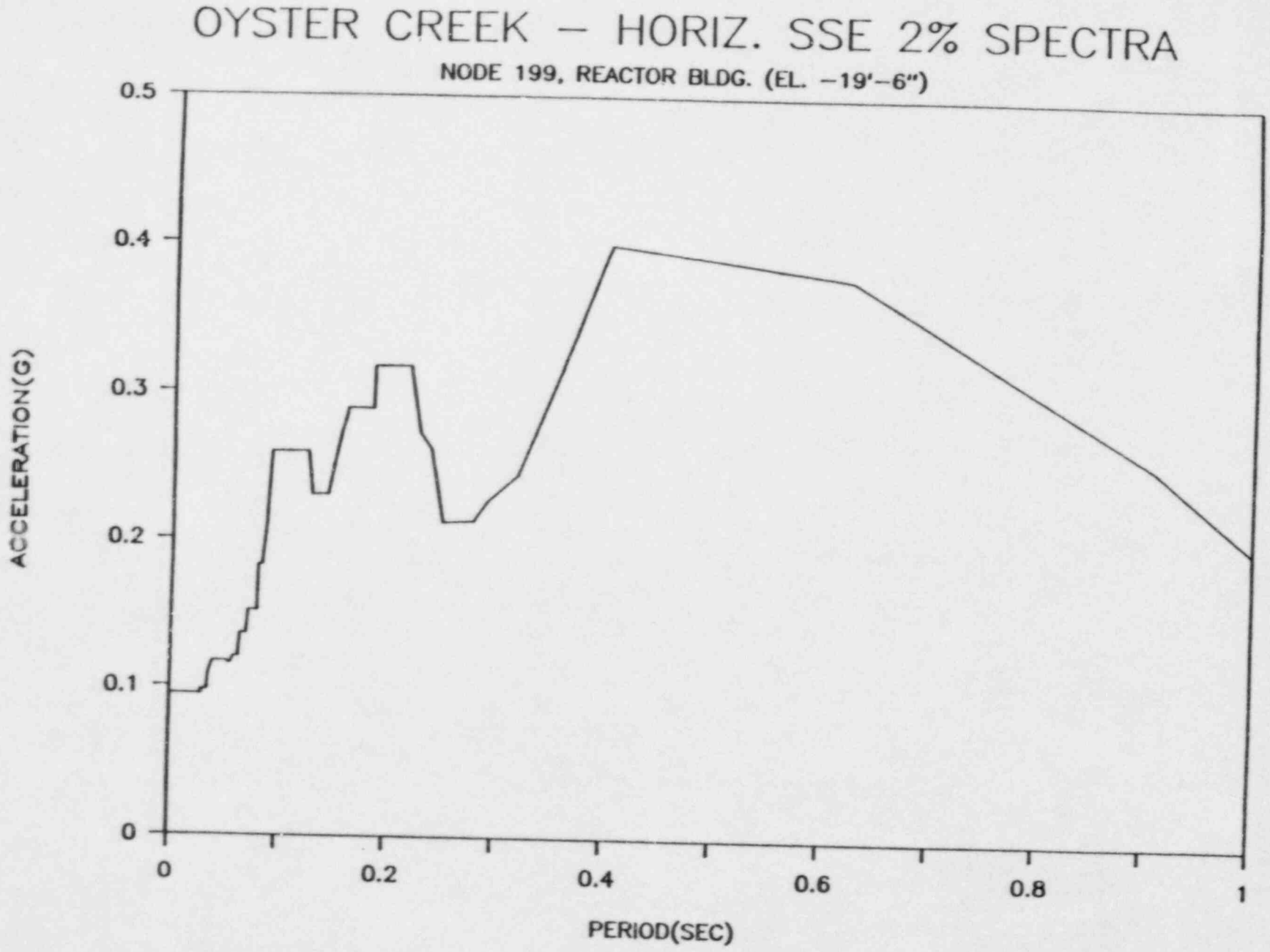

FIGURE 3 SMOOTH/BROADENED HORIZONTAL SSE SPECTRUM AT BASEMAT LEVEL OF THE REACTOR BUILDING

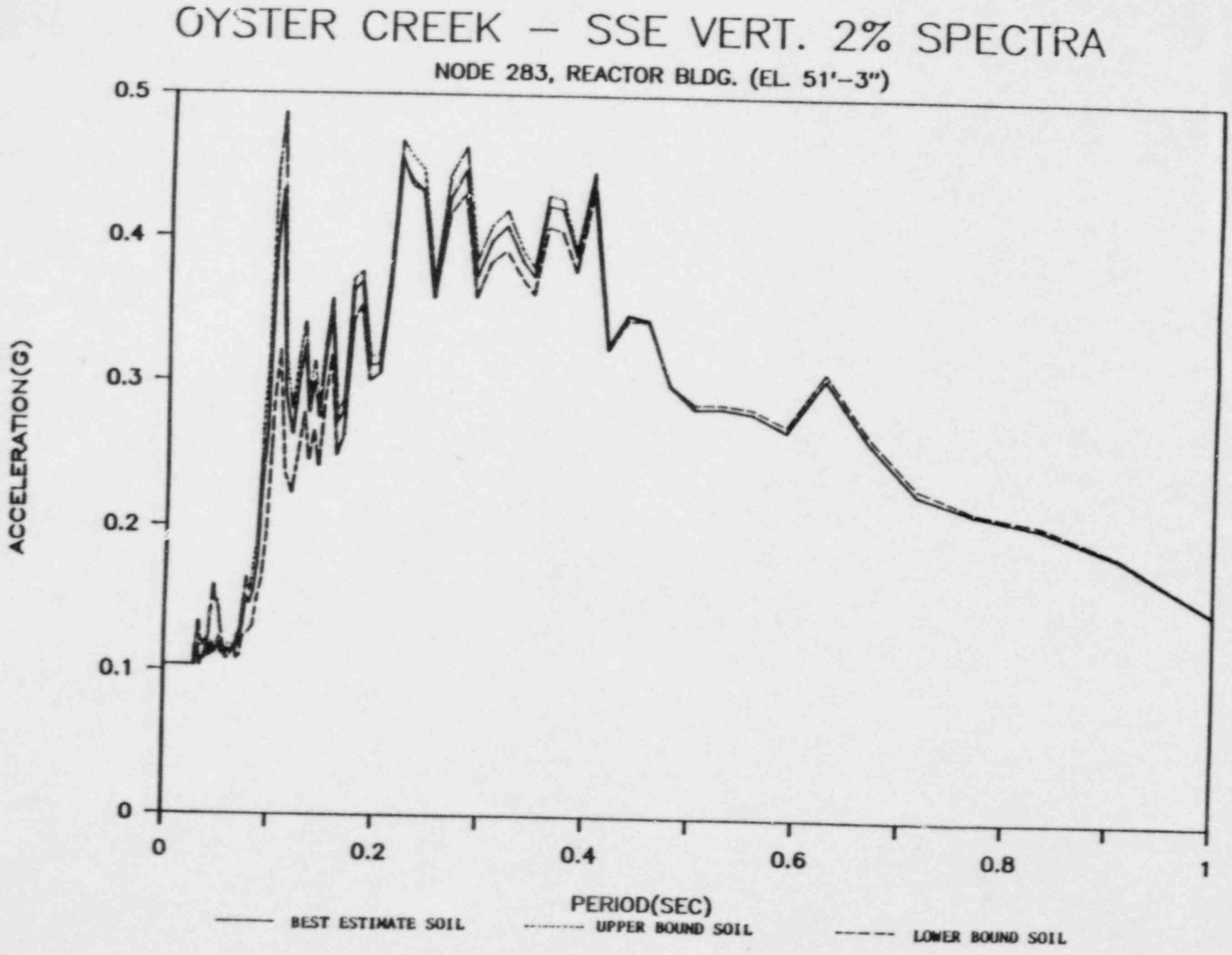

FIGURE 4 RAW VERTICAL SSE SPECTRA FOR SLAB PANEL BETWEEN COLUMN LINES RA/RB AND R3/R4, EL. 51'-3" OF THE REACTOR BUILDING

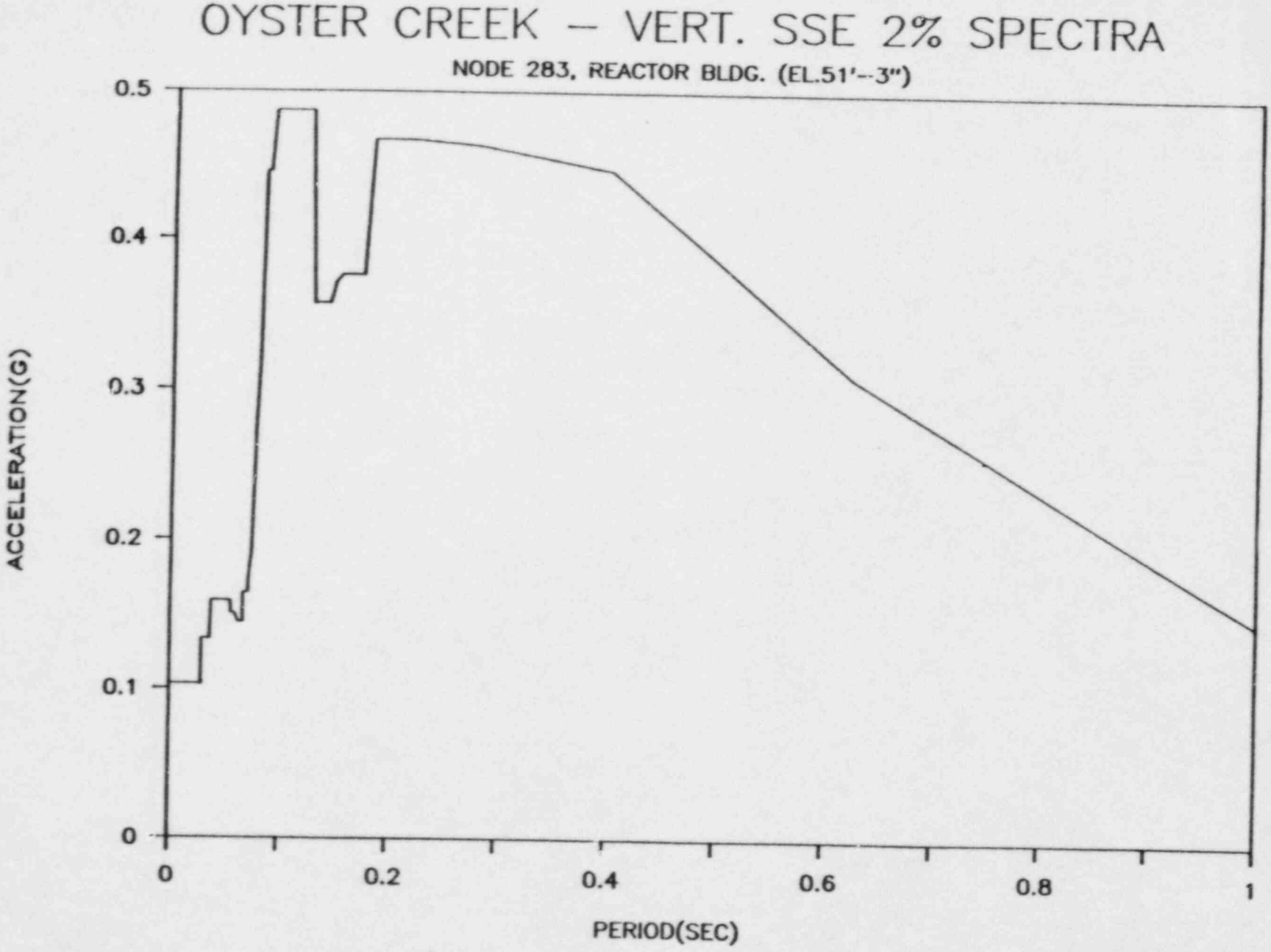

FIGURE 6 SMOOTH/BROADENED VERTICAL SSE SPECTRUM FOR SLAB PANEL BETWEEN COLUMN LINES RA/RB AND R3/R4, EL. 51'-3" OF THE REACTOR BUILDING

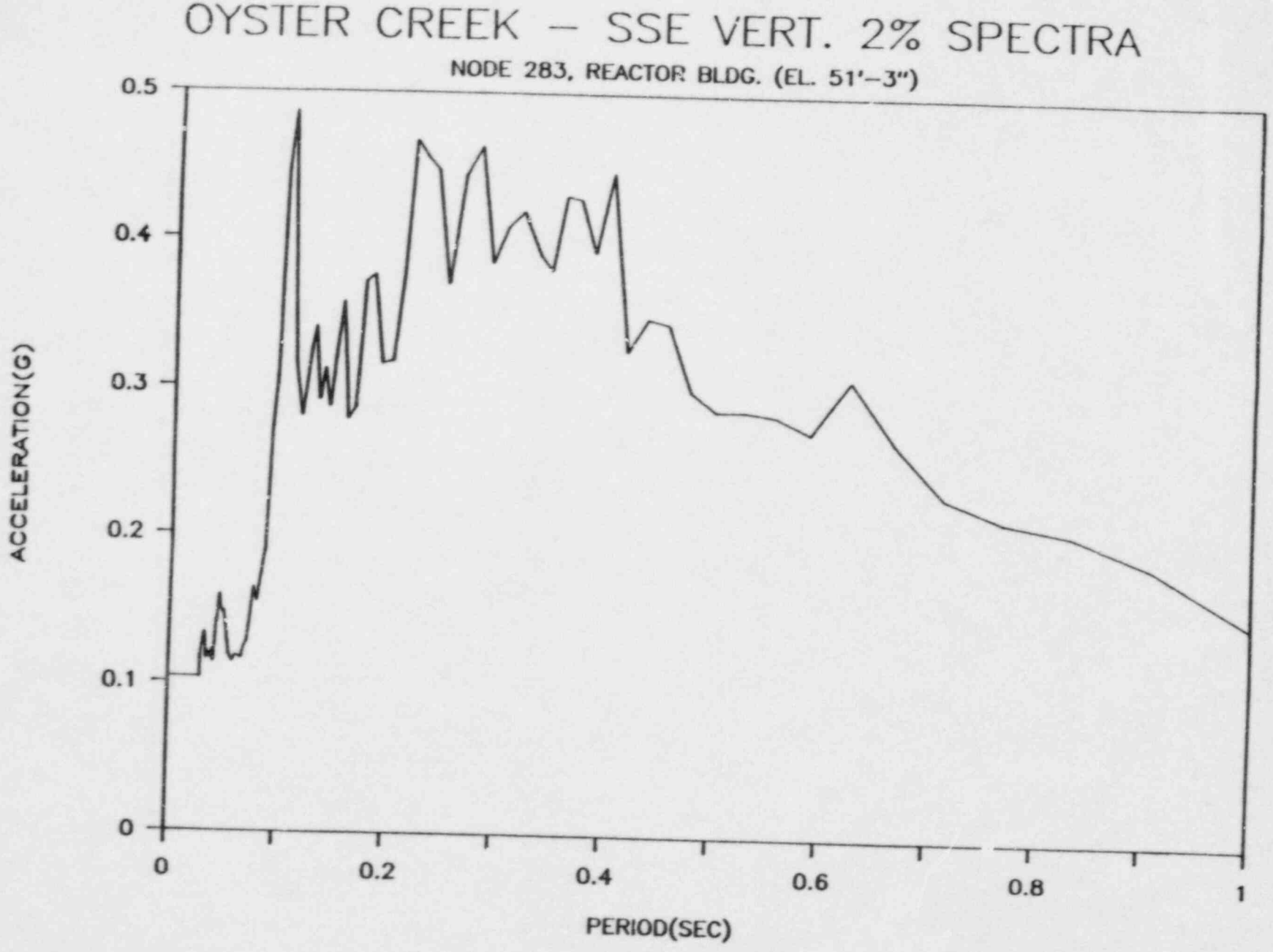

FIGURE 5 RAW ENVELOPED VERTICAL SSE SPECTRUM FOR SLAB PANEL BETWEEN COLUMN LINES RA/RB AND R3/R4, EL. 51'-3" OF THE REACTOR BUILDING

EFFECT OF SATURATED SOIL ON OYSTER CREEK SSI ANALYSIS

Introduction

The following paragraphs describe the soil saturation condition at the Oyster Creek reactor building area and how the saturation effects were considered by URS/Blume in the reactor building SSI analyses.

Condition at Oyster Creek Site

Oyster Creek reactor building is embedded to elevation -29 ft 6 in. The ground surface is at elevation +23 ft 6 in. The water table varies between elevation +3 ft 6 in. to +10 ft as monitored in the well network at the site since 1984 (GPU Memo, 1987). Figure 1 presents the SSI model of the reactor building indicating water table elevations.

Procedure Adopted in Oyster Creek SSI Analysis to Consider Soil Saturation Effects

We have adopted the following procedures to account for soil saturation in SSI analyses for the Oyster Creek plant. We have used field-measured soil properties at the Oyster Creek site, which include effects of soil saturation as manifested in higher P-wave velocities and Poisson's ratio for layers under the water table (Figure 2). In addition, we have monitored P-wave velocities in soil layers in the saturated soil zone of our soil-structure model (Figure 1) during SSI analysis and imposed the condition that the P-wave velocities in these layers will not be less than the P-wave velocity of water. This has been implemented by adjusting the soil Poisson's ratio of these layers using the following equation:

$$\mu = \frac{[1-2(V_s/V_p)^2]}{2[1-(V_s/V_p)^2]}$$

where

- μ = Poisson's ratio to be used for the soil layer in saturated zone
- V_s = Soil layer shear wave velocity
- V_p = P-wave velocity in water

This satisfies the measured field data which indicates P-wave velocity of saturated soil to be close to water P-wave velocity. It is also consistent with theoretical studies of wave propagation in saturated soil medium. Finally, this procedure has been used in SSI analyses of a 1/4-scale containment model embedded in saturated soil and produces good correlation with responses measured in actual earthquakes. These items are discussed in more detail in subsequent sections.

Field Data on Saturated Soil Properties

A large set of in-situ measurements of saturated soil properties using down-hole and cross-hole techniques have been accumulated by Japanese investigators Yokota (1982), Ishihara (1971), Imai (1970), and others. It has been observed in the field surveys that in relatively loose saturated soils, the observed P-wave velocity is close to or slightly higher than the P-wave velocity in water (4,700 fps). In stiffer saturated soils, the P-wave velocity seems to be controlled by the stiffness of the soil frame; i.e., the P-wave travels mainly in the solid phase of the medium at velocities higher than 4,700 fps. It can be inferred from these data that water is the dominant P-wave-transmitting medium in relatively loose saturated soils (i.e., when solid phase P-wave velocity is less than water P-wave velocity). On the other hand, the solid phase (soil frame) becomes the dominant P-wave-transmitting medium in stiff saturated soils.

Similar trends are observed in the field measurements of soil properties reported for the Oyster Creek site (Figure 2). It shows that the P-wave velocity changes from 1,400 fps for the top unsaturated or partially saturated layer to 5,200 fps for the lower fully saturated layer. The Poisson's ratio of the top layer is derived to be 0.39, while that for the second layer is 0.48, reflecting soil saturation effect on P-wave velocity.

Results from Theoretical Studies

The basic theoretical research on wave propagation in a saturated medium was conducted by Biot (1956 and 1962). It was assumed that the saturated soil may be represented by a two-phase system consisting of an elastic skeleton uniformly distributed in space and compressive fluid filling the pores of the skeleton. Soil permeability effects couple the two phases

together. Biot showed that three body waves can propagate in such a medium -- two P-waves and an S-wave. The P-wave of the first kind is identified to be a pure compressional wave. The second kind decays rapidly due to a diffusion-type process.

Studies by Biot and others have concluded that S-waves are hardly influenced by saturation. The P-waves are affected in loose saturated soils, which is consistent with field observations.

Validation of Procedure in Actual SSI Experiments

Electric Power Research Institute (EPRI) is conducting a research program to measure SSI effects in a 1/4-scale model of a reactor containment building subjected to actual earthquakes (Tang, 1987). This 1/4-scale model is set up at Lotung in Taiwan, in an area of high seismicity. To date, 18 earthquakes with Richter magnitudes from 4.5 to 7.0 have been recorded since the seismic instrumentation was put into operation. Two of these earthquakes of magnitudes 6.5 and 7.0, with peak ground acceleration of 0.20g at free field at the site, were used for extensive analyses using various SSI codes.

Lotung site has a deep sandy soil deposit with shear wave velocity varying from 300 fps to 1,000 fps in the top 200-ft soil deposit. The site has saturated soils, as groundwater level is measured at 3-ft depth. The compression wave velocity measurements reflect the saturation effect with almost constant P-wave velocity of 4,500 ft/sec from 20 ft down, with a transition zone near the surface. The effect of soil saturation is reflected in Poisson's ratios which are calculated to be in the 0.45 to 0.49 range.

Several studies were conducted to predict the structural responses of the containment model due to the two earthquakes, using state-of-the-art SSI methodologies including the FLUSH group of programs. In one of the the studies (Tseng, 1987) with the FLUSH program, the Poisson's ratio was adjusted, similar to what is done by URS/Blume for Oyster Creek analyses, to keep the P-wave velocity to a minimum of 4,790 ft/sec. The analyses

results show very good correlation with measured data as presented in Figures 3 and 4.

Another study (Berger, 1987) reported using ALUSH, an axisymmetric version of FLUSH, for the SSI analysis. In this study also, Poisson's ratio was adjusted to maintain P-wave velocity in soil equal to that of water. The correlation with measured data is again very good, as shown in Figures 5 and 6.

Conclusions

Based on the above discussions, the following conclusions may be drawn for Oyster Creek SSI analyses:

- The soil saturation issue has been addressed in the state-of-the-art SSI method for Oyster Creek reactor building SSI analyses.
- The applied methodology is consistent with observed P-wave velocity data from field measurements.
- Application of the same methodology in the EPRI-sponsored Lotung project has yielded analytical results showing good correlation with measured responses in a 1/4-scale reactor containment model situated in a saturated soil site subject to actual earthquakes.

References

Berger, E., H. Fierz, and D. Kluge (1987), "Predictive Response Computations for Vibration Tests and Earthquake of May 29, 1986, Using an Axisymmetric Finite Element Formualtion Based on the Complex Response Method and Comparison with Measurements--A Swiss Contribution," EPRI/NRC/TPC Lotung SSI Workshop, Palo Alto.

Biot, M. A. (1965), "Theory of Propagation of Elastic Waves in a Fluid-Saturated Porous Solid," J. Acoustical Society of America, Vol. 28(2).

Biot, M. A. (1962), "Mechanics of Deformation and Acoustic Propagation in Porous Media." J. Appl. Physics, Vol. 33(4).

GPU Memo (1987), "Transmittal of Groundwater Data for Oyster Creek Site," October 19.

Imai, T., et al. (1970), "Velocities of Elastic Wave Propagation and Mechanical Characteristics of Soft Soil Grounds," Tsuchi to Kiso, Vol. 18, No. 1, pp 17-22.

Ishihara, K. (1971), "On Longitudinal Wave Velocity and Poisson's Ratio in Saturated Solids," Proc. Fourth Asian Regional Conf. on Soil Mech. and Found. Engineering," Vol. 1, pp. 197-201, Bangkok, Thailand.

Tang, H. T. (1987), "Large-scale Soil-structure Interaction," NP-5513-SR, EPRI, Palo Alto, California.

Tseng, W. S., et al. (1987), "Soil-structure Interaction Analyses of Quarter-Scale Containment Model Experiment in Lotung, Taiwan," EPRI/NJRC/TPC Lotung SSI Workshop, Palo Alto.

Yokota, K., et al. (1982), "Geotechnical and Geophysical Methods for Evaluating Dynamic Soil Properties at Various Sites in Japan," Proc. third International Conference on Microzonation, pp. 1129-1144, Seattle, U.S.A.

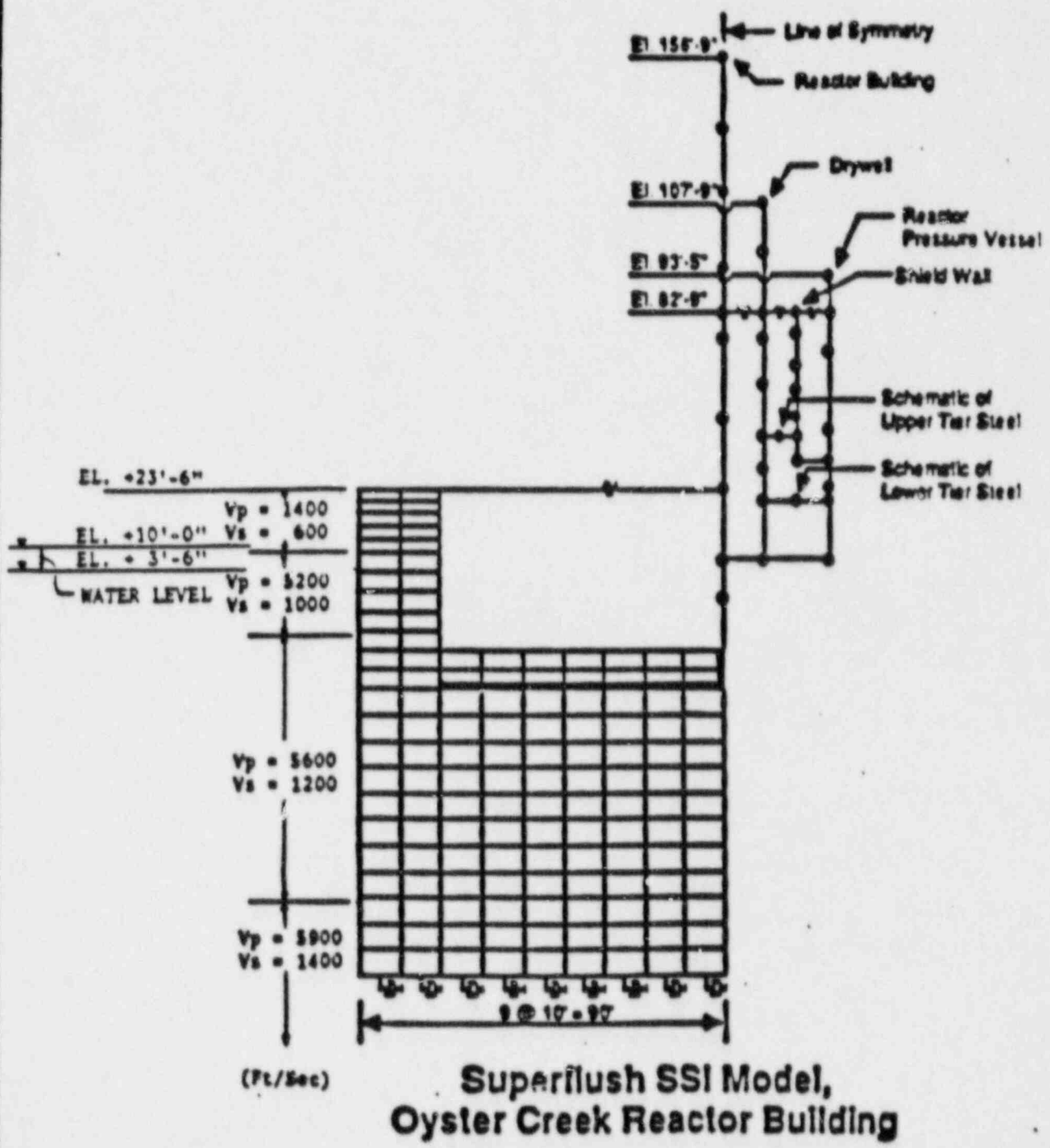

Superflush SSI Model, Oyster Creek Reactor Building

Figure 1.

MEASURED P-WAVE VELOCITY Vp (ft/sec)	REQUIRED SHEAR WAVE VELOCITY Vs (ft/sec)	POISSON'S RATIO	SHEAR MODULUS (KSF)			LAYER DEPTH (ft)
			BEST ESTIMATE	UPPER BOUND	LOWER BOUND	
1400	600	0.39	1342	1678	895	15
5200	1800	0.48	3727	4659	2485	25
5600	1200	0.48	5366	6708	3577	65
5900	1400	0.47	7384	9130	4869	35

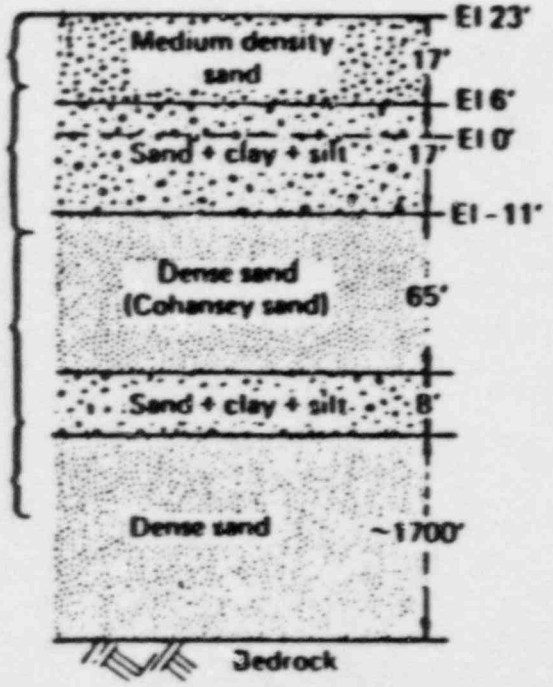

Note: Water table varies between El. +3.5' to +10.0'

FIGURE 2: SOIL SHEAR WAVE VELOCITY PROFILE AT OYSTER CREEK PLANT

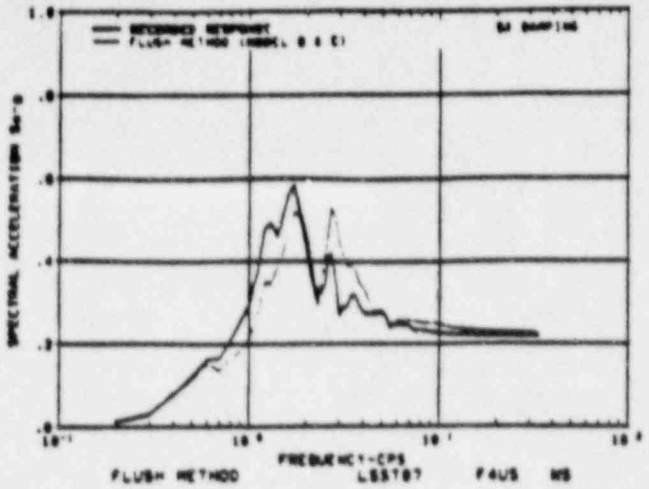

a. Top of Structure, N/S Direction

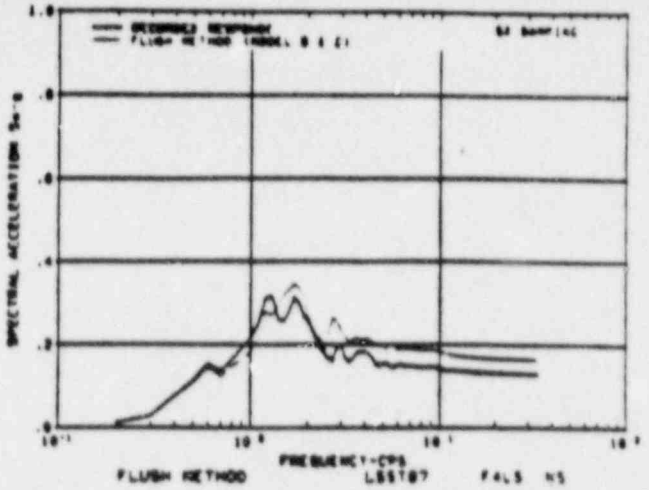

d. Basemat of Structure, N/S Direction

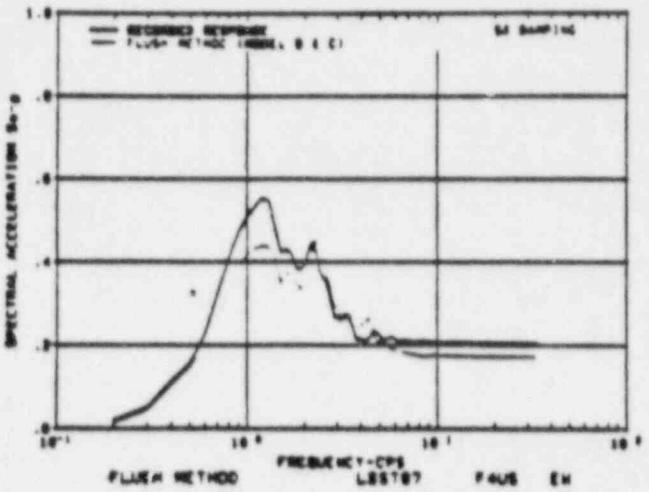

b. Top of Structure, E/W Direction

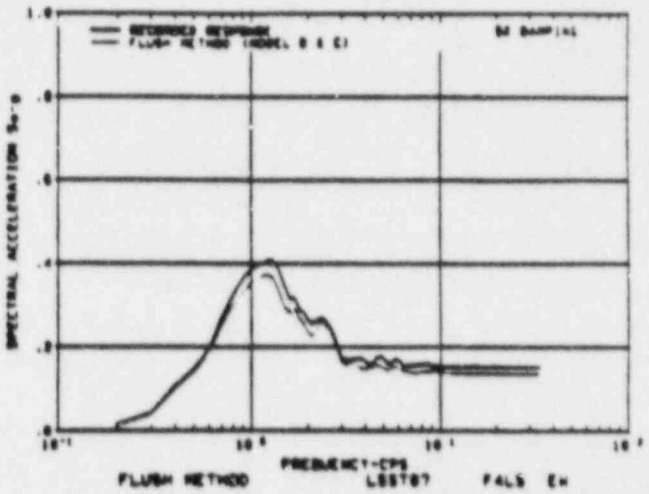

e. Basemat of Structure, E/W Direction

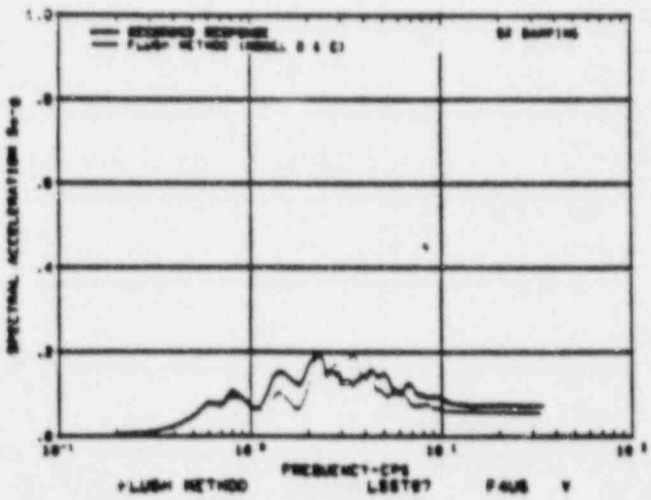

c. Top of Structure, Vertical Direction

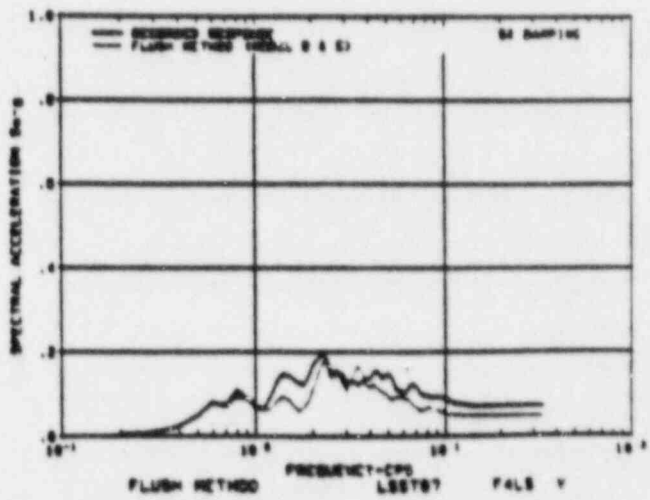

f. Basemat of Structure, Vertical Direction

Figure 3. Comparison of Measured and FLUSH Computed Response Spectra at the Top and Basemat of the 1/4 Scale Containment Model, Lotung Study (May 20, 1986 Earthquake, 0.20g ZPA)

URS/Blume

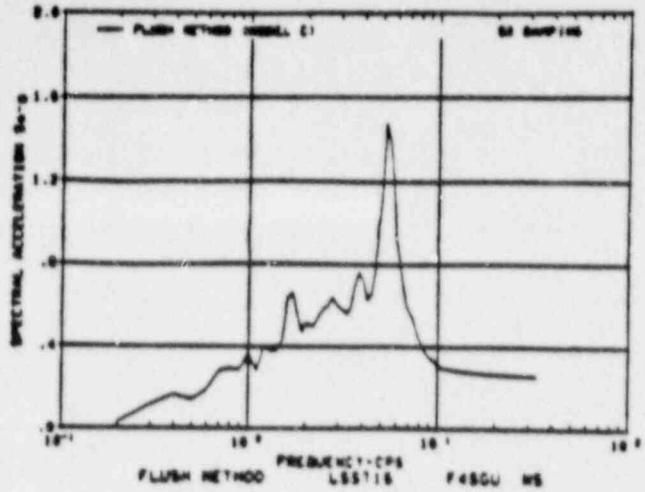

a. Top of Structure, N/S Direction

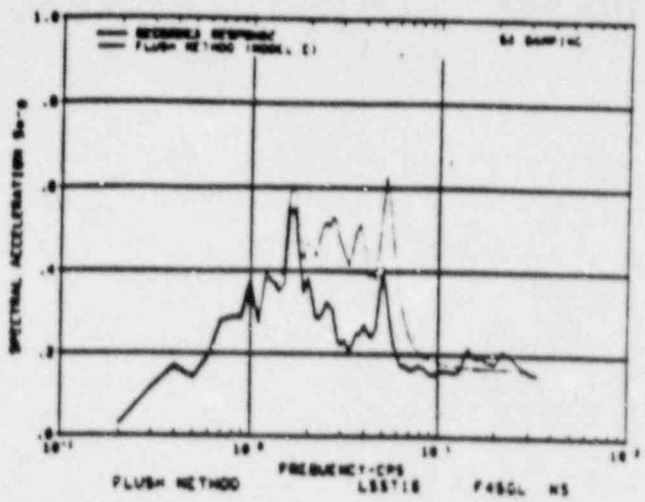

d. Basemat of Structure, N/S Direction

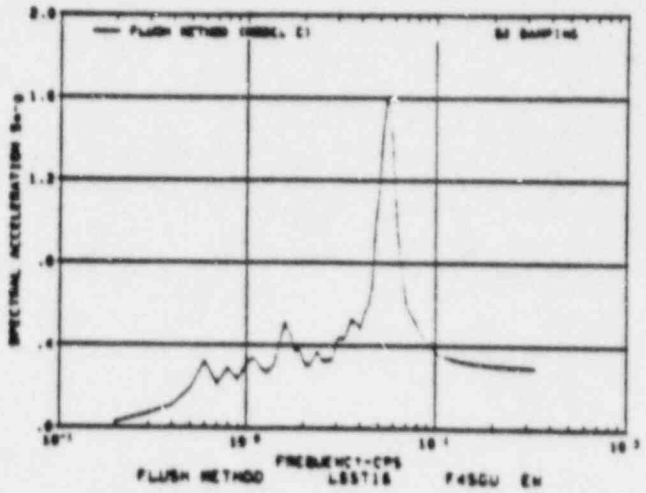

b. Top of Structure, E/W Direction

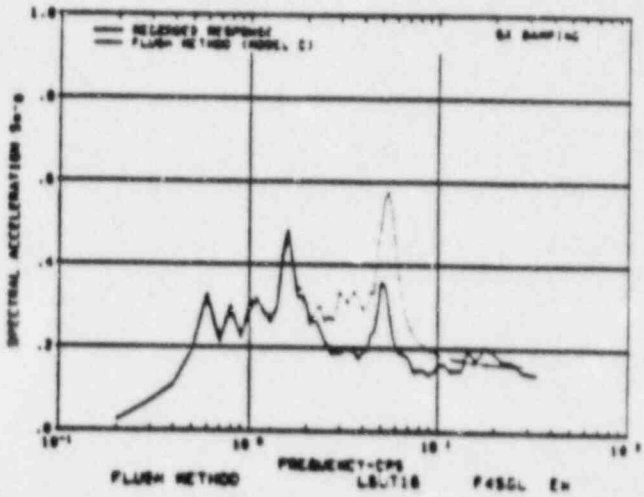

e. Basemat of Structure, E/W Direction

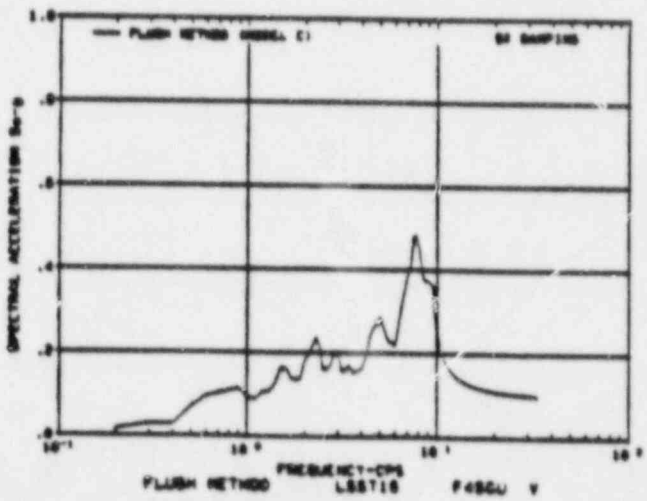

c. Top of Structure, Vertical Direction

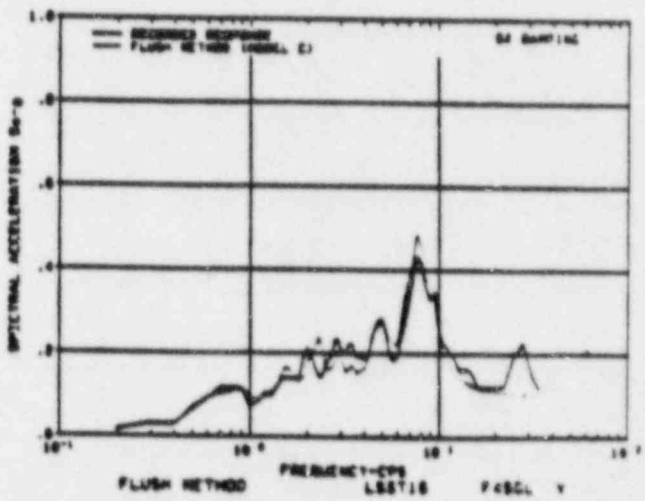

f. Basemat of Structure, Vertical Direction

Figure 4. Comparison of Measured and FLUSH Computed Response Spectra at the Top and Basemat of the 1/4 Scale Containment Model, Lotung Study (Nov. 14, 1986 Earthquake)

URS/Blume

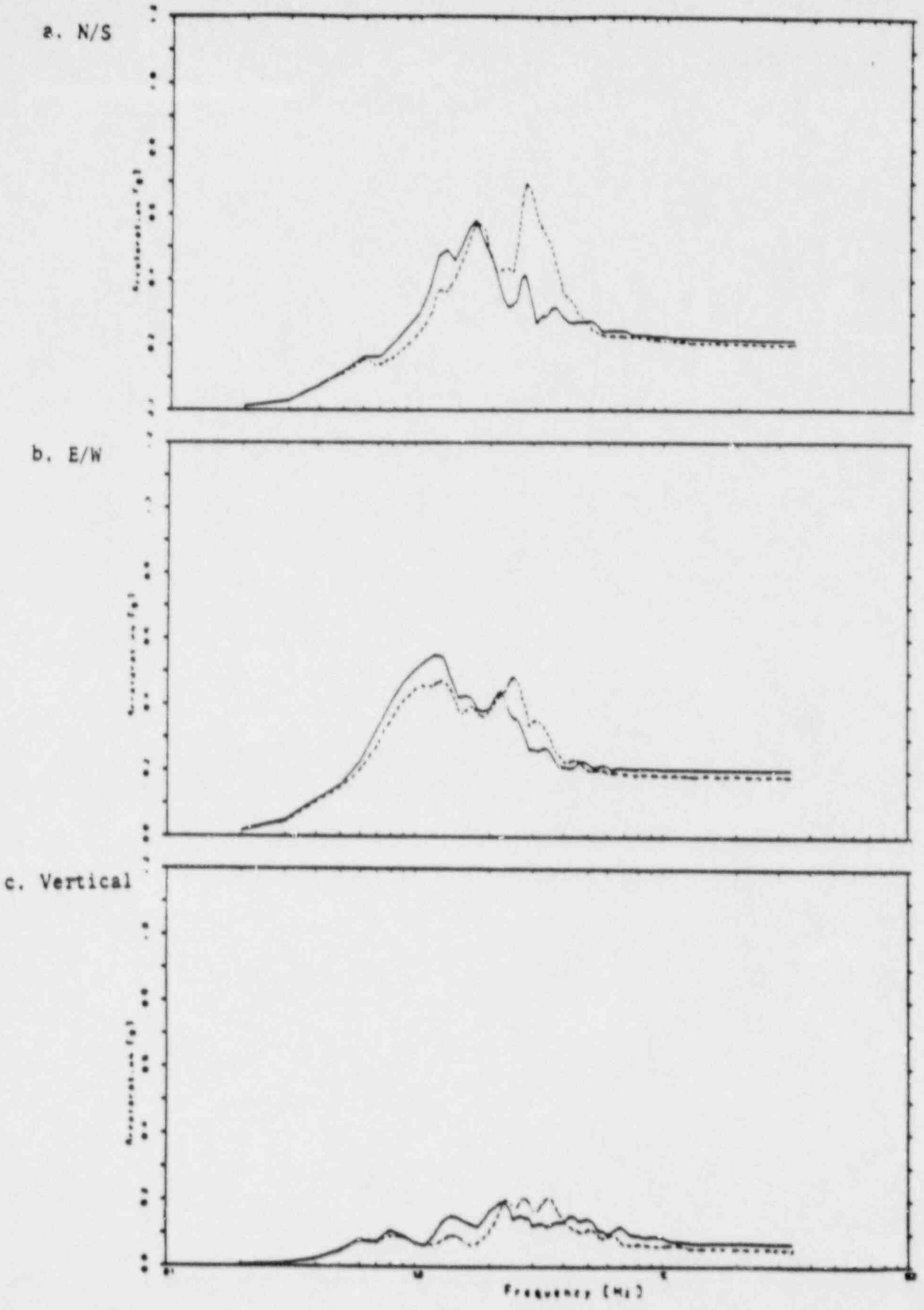

Figure 5. Measured (——) and Predicted (----) Acceleration Response Spectra on Top of Structure (May 20, 1986 Earthquake)

URS/Blume

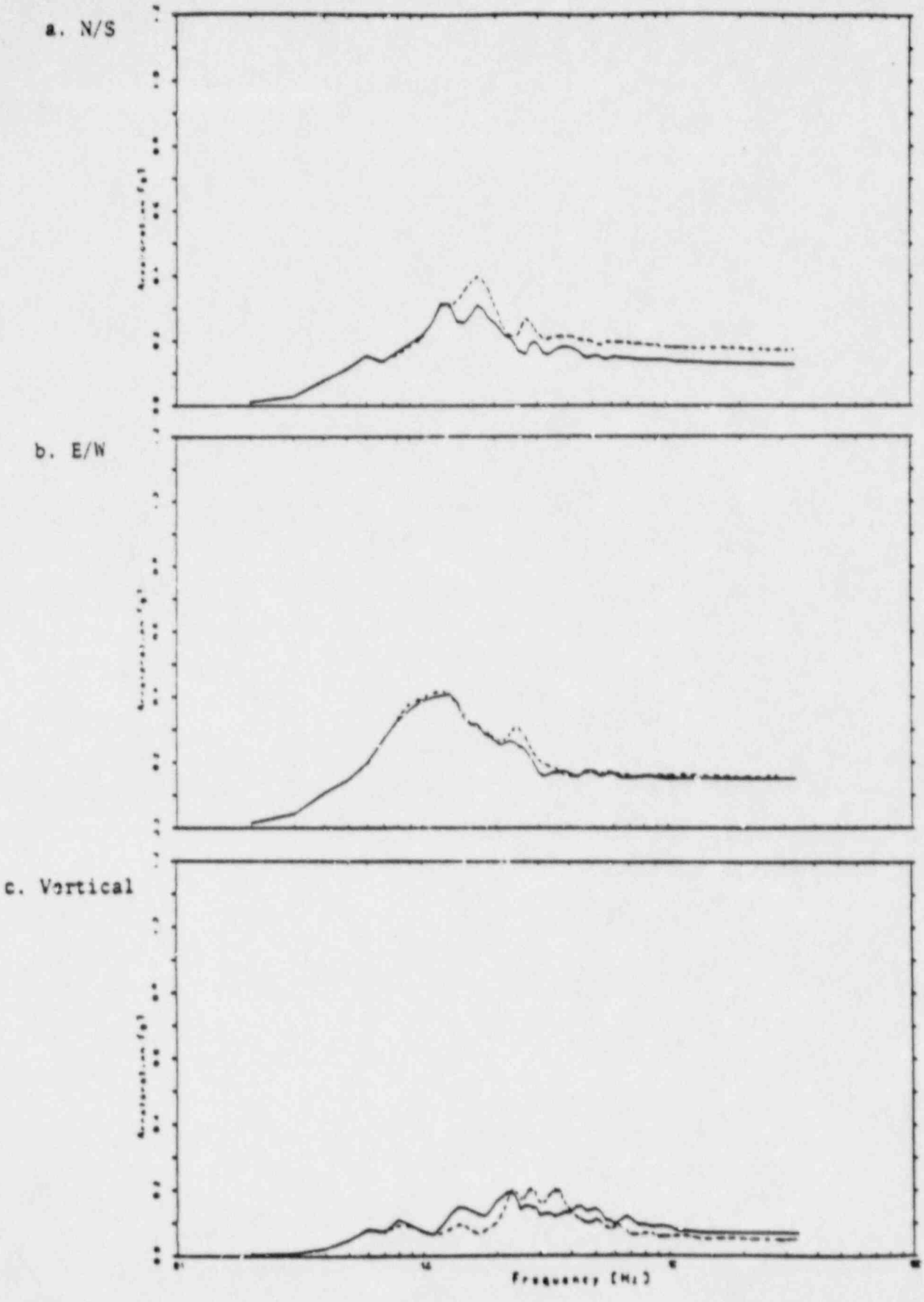

Figure 6. Measured (——) and Predicted (----) Acceleration Response Spectra at Basemat of Structure (May 20, 1980 Earthquake)

sophisticated forms of half-space analysis which introduce the essential concepts of a complete interaction approach are developed, it seems that both methods of analysis may ultimately develop to the point in which they give similar results for embedded structures at comparable costs.

A major factor contributing to the continuing debate concerning the merits of any form of analytical approach has been the total absence of recorded field performance by which the adequacy of such an approach might be judged—making it necessary for engineers to adopt one approach or the other on the basis of their personal appraisals of factors such as the degree of sophistication of the analysis, the potential savings in design costs, the potential losses in overall project costs, their degree of understanding of the nature of the phenomena and principles involved, etc. In the absence of known field performance, all reasonable suggestions for design approaches must be considered potentially applicable, and considerable insight, wisdom, and intellectual honesty

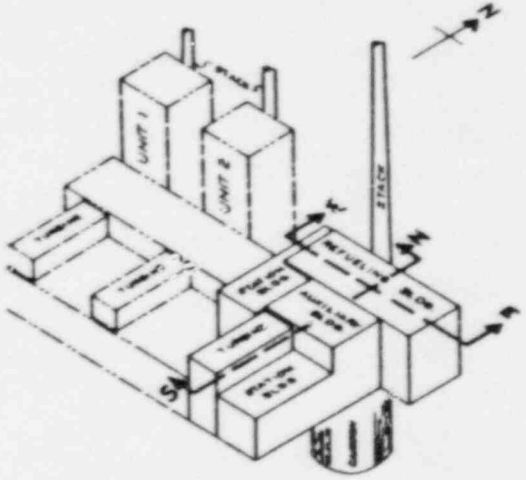

FIG. 1.—General View of Humboldt Power Plant (After Bechtel Co.)

are required to select a design method that offers the greatest potential for combining adequate safety for critical structures with reasonable overall economy in the cost of the completed facility. It is for these reasons that the motions recorded at the Humboldt Bay Power Plant in the Ferndale earthquake of June 7, 1975 are of major significance.

A general view of the plant is shown in Fig. 1. Units 1 and 2 are fossil fuel units whereas Unit 3 is nuclear. The buried reactor structure within the Refueling Building of Unit 3 consists of a massive concrete caisson embedded at a depth of approx 85 ft (26 m) below the ground surface. The various surrounding structures are lightweight structures and are founded at or close to the ground surface. The facility was constructed in 1963 and has been operating satisfactorily since that time.

Strong motion instruments at the plant have been in operation since September, 1971. These are located at elevation +12 (plant grade level) and elevation −66

in the Refueling Building, and in a Storage Building (elevation +12) some 330 ft (100 m) south of the Refueling Building.

The June 7, 1975 earthquake (magnitude approx 5.5 on the Richter scale) had its epicenter approx 15 miles south of the plant site and triggered strong

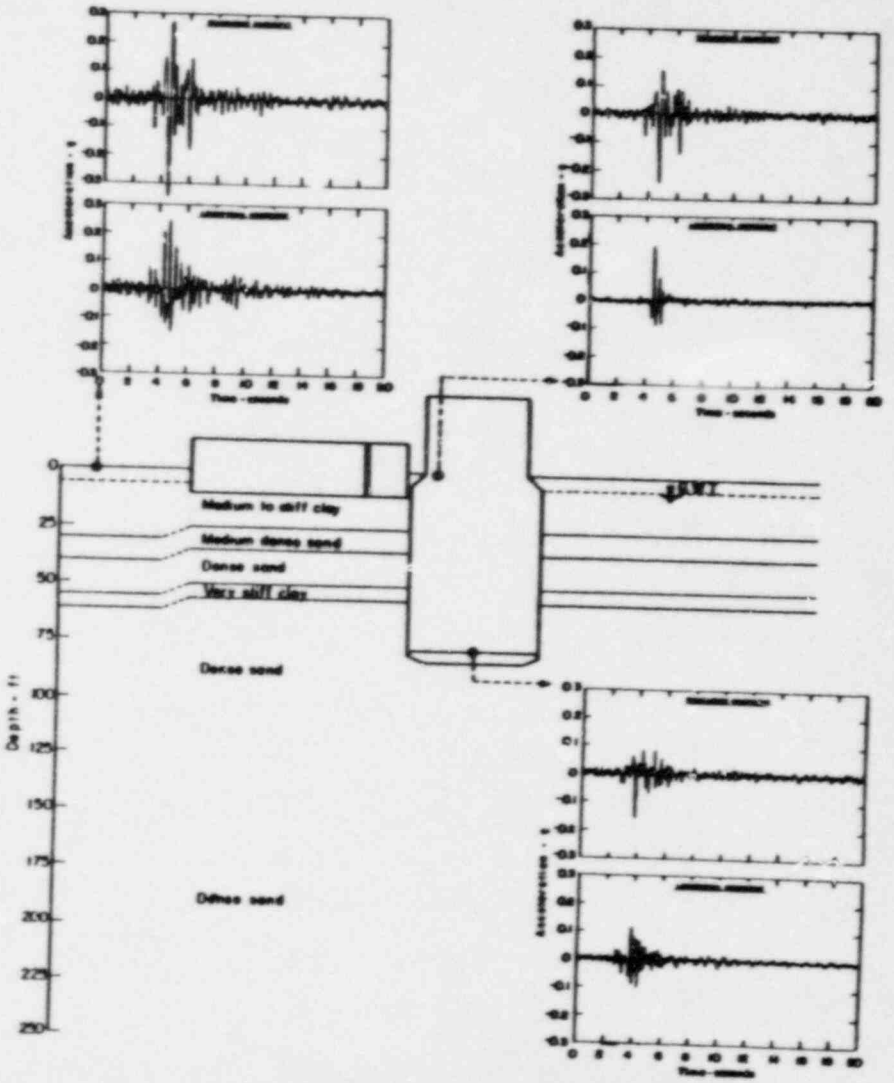

FIG. 2.—Ground Motion Records at Humboldt Bay Power Plant (1 ft = 0.305 m)

motion instruments in the surrounding area, including those located at the Humboldt Bay Plant. The earthquake records obtained at the Humboldt Plant are shown in Fig. 2. Although the duration of strong shaking was only approx 3 sec–5 sec, the baseline-corrected peak accelerations developed in the free

TORSIONAL EFFECTS ON STRUCTURE

Introduction

The following paragraphs describe the study done by URS/Blume to assess the torsional effects of Oyster Creek reactor building mathematical model on the computed horizontal floor response spectra (FRS).

Background

A lumped-mass stick model (Figure 1) was developed to compute seismic FRS for Oyster Creek reactor building. The masses of a floor and of the top and bottom walls tributary to the floor are lumped at that floor. The vertical beams between the floors represent the lateral stiffness of the walls between the floors. Mass and stiffness calculations for the reactor building has shown that the centers of mass at each floor and the centers of rigidity between the floors do not coincide. This is due to some asymmetry in mass and stiffness distribution in the reactor building.

However, the eccentricities between the centers of masses and rigidities in the Oyster Creek reactor building are small, and frequency calculations showed that the mass participation in torsional modes are insignificant compared to the horizontal modes. In addition, the building dynamic properties in the east-west and north-south directions are very similar. The computed FRS in the east-west and north-south directions from the mathematical model of Figure 1 were very close. As a result, it was determined that a 2-dimensional representation of the reactor building model will be able to capture accurately the seismic responses. Such a model was used for SSI calculations and FRS generation. Horizontal FRS computed from such a model does not include the horizontal component that may occur due to torsion of the floor mass about the center of the rigidity due to eccentricities between the centers of mass and rigidity. The NRC staff requested a study to demonstrate that the horizontal FRS component due to torsion is insignificant as assumed in the Oyster Creek reactor building FRS generation.

Parametric Study

To study the effects of the torsional component on horizontal FRS, two computer runs were made with the lumped-mass mathematical model of the reactor building (Figure 1). The first computer run computed the total horizontal FRS at an extreme corner point on the operating floor slab (El. 119 ft 3 in.) from the slab center line (70 ft in west and 70 ft in south direction) considering both translation and torsion of the structure. This is the worst case slab location for torsion. The second run did not consider any contribution to the horizontal FRS due to torsion of the structure. The resultant FRS for 5% damping are presented in Figure 2. It shows insignificant (5% or less) contribution of torsion on the horizontal FRS of Oyster Creek reactor building.

Conclusion

The torsional effects, due to mass and stiffness asymmetry of Oyster Creek reactor building, have insignificant impact on total horizontal FRS generated for the building.

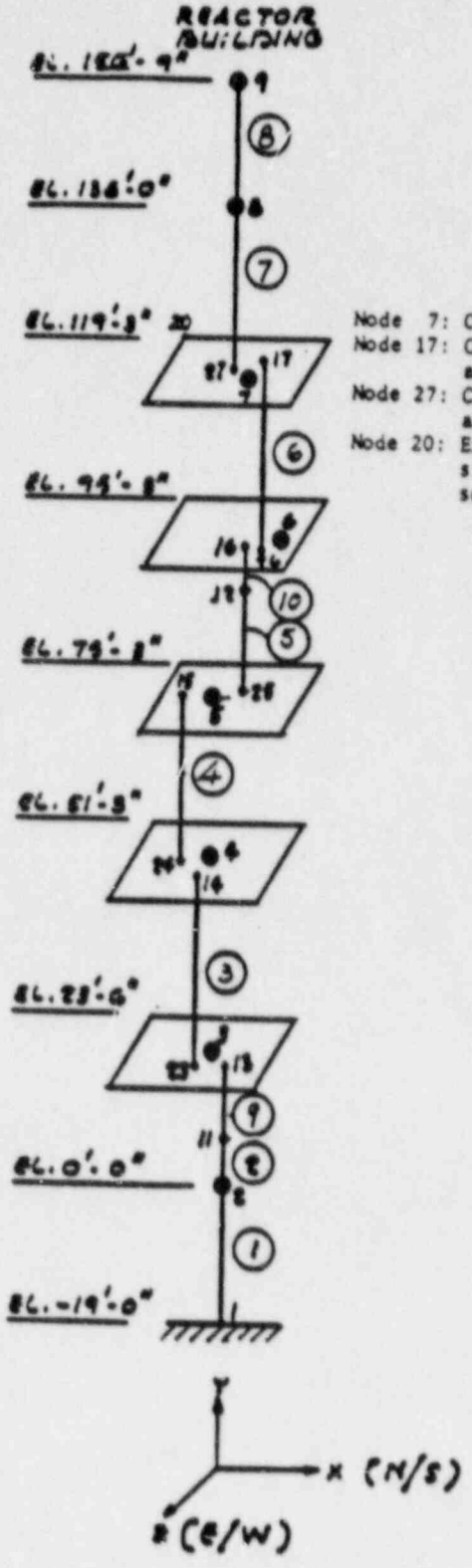

Figure 1 3-D Lumped-mass Model of Reactor Building

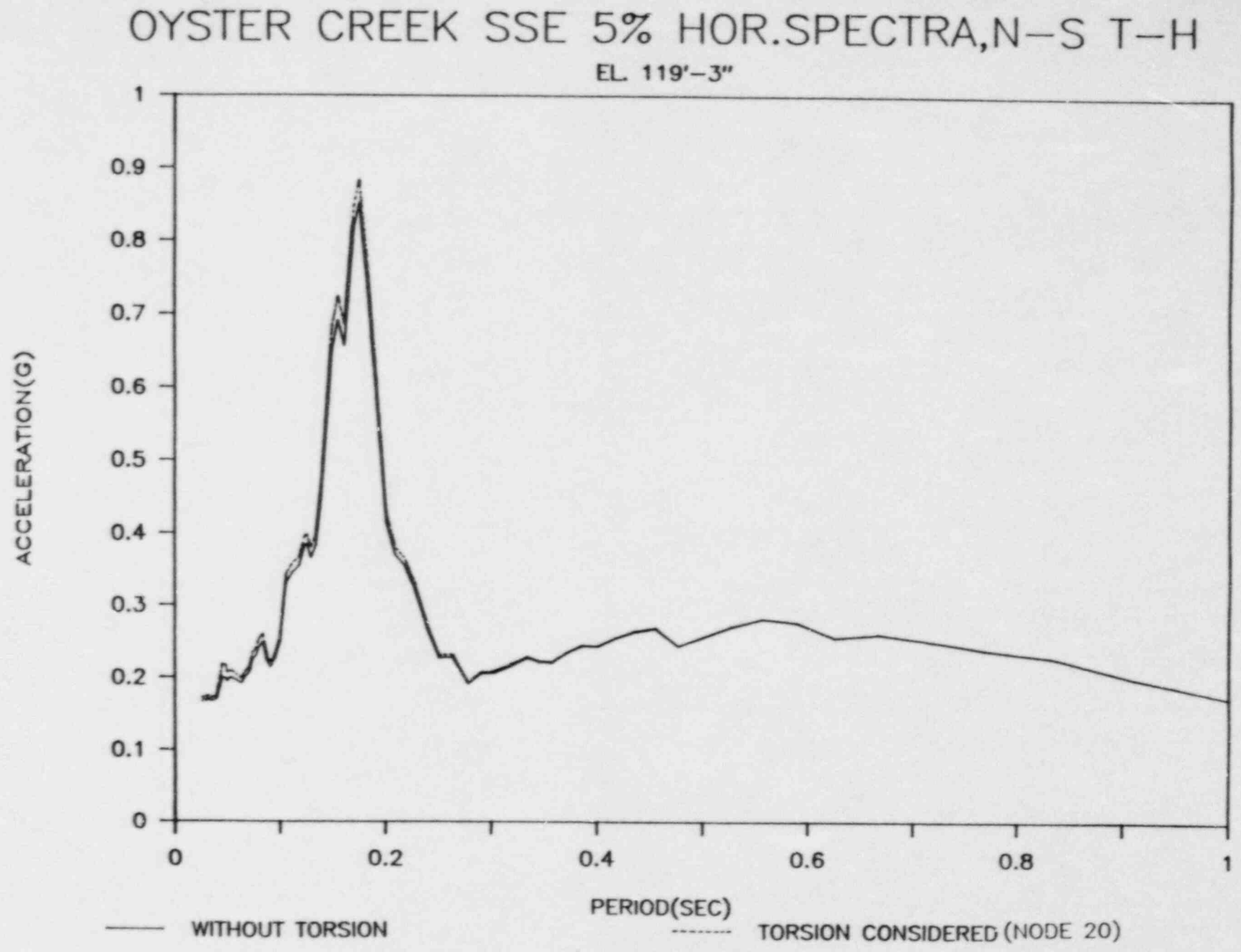

Figure 2 Floor Response Spectra at Operating Floor. (El. +119'-3")